

Effect of DTM resolution on the determination of slope values in an upland catchment using different computational algorithms

Damian Badora, Rafał Wawer

Department of Soil Science Erosion and Land Conservation
Institute of Soil Science and Plant Cultivation – State Research Institute
ul. Czartoryskich 8, 24-100 Puławy, POLAND

Abstract. This paper presents the results of determining slope values using seven different DTM (digital terrain model) methods for different resolutions: 1, 5, 10, 30, 90 meters for the Bystra catchment area. After calculating the slopes using different methods for different resolutions, the slope values were grouped into following slope range classes: 0.00°–2.99°, 3.00°–5.99°, 6.00°–9.99°, 10.00°–14.99° and ≥15°. The results of slope calculations were compared with geodetic field measurements at the slopes of the Esterka castle in Bochoznica, which is located in the Bystra catchment area. It was found that the good reproduction of the actual terrain relief, represented by the 1 m resolution DTM, deteriorates significantly starting from 30 m resolution. The method for determining terrain slopes that most accurately represents the true relief variability is Third-order Infinite Method for Calculating Slope (M3) (Horn, 1981). This method is considered more suitable for varied landscape relief. But the 2nd Degree Polynomial Adjustment method (Zevenbergen et al., 1987) is recommended for flat terrain. The results of the analyses are crucial for determining the minimum quality of DTM data.

In this study, high resolution data (less than 30 m) were found to be suitable for analysis and interpretation of terrain slopes in a small upland catchment. Due to the optimum processing speed of the data and the very good representation of the terrain, a resolution of 5 m seems to be the optimum solution that can be used for further studies of the Bystra river catchment. The results of the study show what resolution of DTM should be used for other studies: morphometric, geomorphological or hydrological of small catchments, where the quality of results is important, e.g. in accurate water balance analysis of catchments or soil erosion analysis in agriculture.

Keywords: terrain slope, DTM, resolution of the DTM

INTRODUCTION

This paper deals with the impact of the resolution of the Digital Terrain Model (DTM) on the calculation of the terrain slope of the Bystra River catchment – by seven computational methods. The DTM is a digital representa-

tion of terrain elevation information, which is in the form of a two-dimensional matrix sampled against an elevation datum (Moore et al., 1991). One of the primary processes of DTM processing is the calculation of terrain slopes. This parameter showing the relief of the land surface is an important factor in morphometric studies, hydrology and geomorphology.

Land relief has a very strong influence on the type and intensity of physical and geographic processes, primarily morphological, as well as on the quality of agricultural production space, construction, communication. The relief of the land surface directly affects the degree of difficulty of tillage, the intensity of soil erosion, which translates into the organisation of agricultural production (Sałata, 2015). On the other hand, the slope of the terrain influences the intensity of erosion processes, differentiates agro-ecological conditions, limits agro-technical treatments and conditions the occurrence of specific soil-agricultural complexes (Sałata, 2015). In the 1980s and 1990s, large-scale studies on soil erosion extents, intensity and consequences to agricultural production were carried out. A number of scientific centres participated. The studies showed that there is a decline in the productivity of agriculturally used soils (Zachar, 1982). Surface water erosion and gully erosion is an important threat for Polish areas (Józefaciuk, Józefaciuk, 1979, 1992a; Józefaciuk, Józefaciuk, 1992b). It causes negative natural and economic impacts (Nowocień, 2008; Wawer, Nowocień, 2018).

A problem related to highly diverse terrain's relief, especially in upland areas, is the rational use of space in the spatial planning process, which is not possible without taking geomorphological considerations into account. One of the solutions to this problem is the use of morphometric maps, which show relief parameters (mainly slopes) in a numerical way, and morphodynamic maps, which show current geological-geomorphological processes (Baran-Zgłobicka et al., 2011). With the advent of DTMs, the use of geomorphometry has expanded. DTM-based geomorphometry allows rapid determination of morphometric pa-

Corresponding author:

Damian Badora
e-mail: dbadora@gmail.com
phone: +48 693 021 525

rameters for different areas compared to manual methods (Wieczorek et al., 2011).

The basic DTM in Poland is a continuously updated model in a 1 m × 1 m grid based on LIDAR (Light Detection and Ranging) data, and stereoscopic survey data for urban areas. LIDAR data is derived from Airborne Laser Scanning (ALS) (CODGiK, 2013).

An important advantage of DTM created from LIDAR laser scanning is the measurement of relief in areas inaccessible to other measurement methods. These include areas with dense vegetation, flooded areas, areas that are difficult to access (Stateczny, Łogasz, 2007). There are two basic types of DTM based on different geometric structures: the GRID pseudo-raster model and the TIN (Triangular Irregular Network) model. GRID is a model of a regular grid of squares with skeleton points and lines. It is created by interpolating measured data or using the TIN model. The TIN model takes the form of an irregular triangle network. The triangle network is created by triangulating the heights of points that are measured directly in the field or indirectly by remote sensing methods (Hejmanowska, 2007). One of the main limitations of the GRID model is the unreal representation of relief discontinuities, e.g. rock cliffs, trenches, gully slopes. In such a case, the TIN model, which better represents the reality of varied relief, should be used for hydrological or geomorphological purposes. The advantage of DTM using the TIN model is the variability of spatial resolution, which allows for efficient data storage. On the other hand, the disadvantage of the TIN model is the increased complexity of the data structures and algorithms used, which causes the greatest limitation in the use of this model. This gives a great advantage to the GRID model in various research fields, through the simplicity of the model and computational efficiency (Szczepaniak-Kołtun, 2016). An important aspect when using DTM is also its quality and accuracy, which affects the reliability of the results of GIS (Geographic Information Systems) analyses (Hejmanowska et al., 2008). The quality of DTM can be degraded by reducing the resolution of the model. Such an operation speeds up the processing of the resulting raster in GIS software. On the other hand, it can significantly reduce the quality of the acquired results. This is reflected, for example, in hydrology, where different resolution affects the accuracy of watercourse line extraction (Szczepaniak-Kołtun, 2016), as well as in the creation of catchment and sub-catchment areas. Resolution and elevation data acquisition methods also affect the accuracy of the DTM and the slope model (Burdziej, Kunz, 2006).

The aim of this paper is to compare the results of determining slope values using seven different methods for different raster grid resolutions: 1, 5, 10, 30, 90 meters on the basis of standardised 1 m × 1 m resolution grid DTM sheets obtained from the Central Geodetic and Cartographic Documentation Centre (CODGiK, 2013). The results of the slope calculations were compared with geodetic field

measurements of slopes in the vicinity of the Esterka castle in Bochothnica (located in the Bystra catchment area).

In this paper, an attempt has been made to find appropriate resolutions to determine the minimum quality of DTM data that can be used for other studies: morphometric, geomorphological or hydrological studies of small catchments, where the quality of the results is important, e.g. in the accurate analysis of the water balance of a catchment or in the analysis of soil erosion in agriculture, the assessment of which, in the light of recent climate change studies, is very important (Badora et al., 2022).

STUDY AREA

Bystra River (Figure 1) is a right tributary of the Vistula with a catchment of 298 square km. It is approximately 36 km long and flows through Nałęczów, Wąwolnica, Celejów, Bochothnica in the Lublin Province. The study area was chosen because of its varied relief (numerous gorges) and the upland nature of the catchment.

METHODS

The different methods of determining slopes

In the first stage of the paper, rasters of the slope gradients of the Bystra river catchment were generated using seven methods of calculating slope gradient for resolutions of 1, 5, 10, 30 and 90 meters. All DTMs with resolution above 1 m were generated from the 1 m DTM using nearest neighbour resampling method. The slope calculation methods tested in the paper use pixel values in a 3×3 matrix, and the calculated result is assigned to the central pixel. In the next chapter, a statistical analysis of the results of the different methods for determining terrain slopes from DTMs with different resolutions is carried out.

After calculating the slope gradients using different methods for different resolutions, the following terrain slope ranges were created: 0.00°–2.99°, 3.00°–5.99°, 6.00°–9.99°, 10.00°–14.99° and ≥15° into which the corresponding pixels were included. The number of pixels in a given range of terrain slopes was then analysed for different resolutions. The calculation of the slope gradients based on the DTM can be done using a number of software packages on the market. In this article, seven different methods for the calculation of terrain slopes were proceeded in SAGA scientific GIS software package. The abbreviated names of the methods M1 to M7 were adopted for further analysis (Table 1).

The first Maximum Slope (M1) method, used by Travis (Travis et al., 1975), involves calculating the slope for pixel Z_5 (Figure 2) relative to each of its eight neighbouring pixels, using the absolute value of the height difference between Z_5 and its neighbours divided by ΔS . The maximum

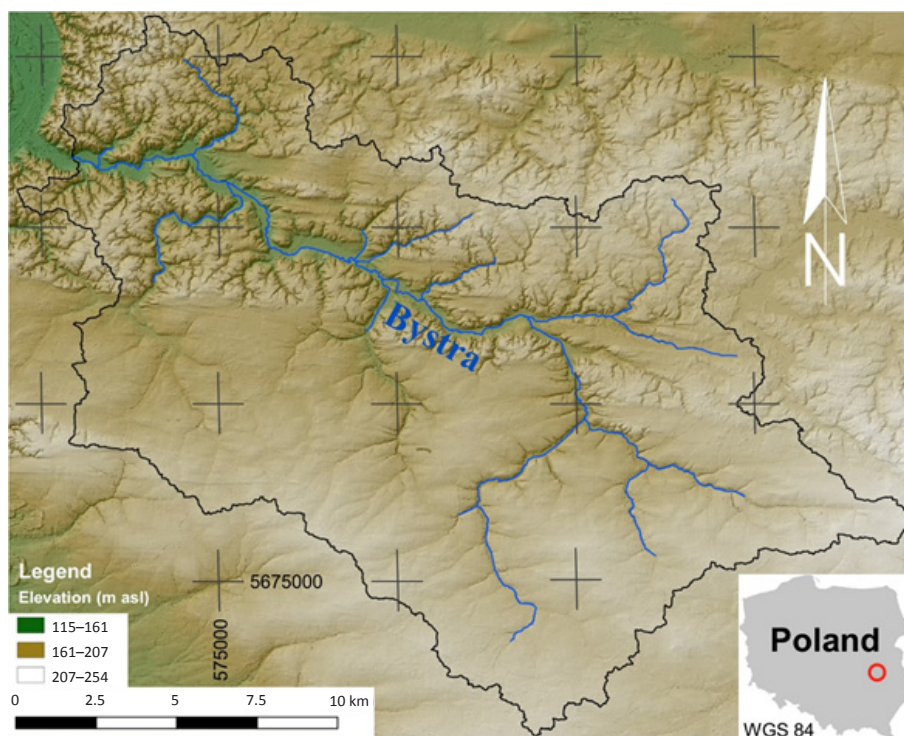


Figure 1. Catchment Bystra river (authors' own study).

Table 1. Summary of slope calculation methods (authors' own study).

| SAGA GIS name | Original name | Source | Abbreviation |
|------------------------------------|---|---------------------------|--------------|
| Maximum Slope | Maximum Max (Tang, Pilesjö, 2011) or Maximum Slope (García Rodríguez, Gimenez Suarez, 2010) | Travis et al., 1975 | M1 |
| Maximum Triangle Slope | D-infinity (Nicotina et al., 2011) or Slope on a Single Facet (Tarboton, 1997) or Maximum Slope by Triangles (García Rodríguez, Gimenez Suarez, 2010) | Tarboton, 1997 | M2 |
| Least Squares or Best Fitted Plane | 8 Neighbors Weighted Horn (Slope algorithms, 2015) or Third-order Infinite Method for Calculating Slope (Weih, Mattson, 2004) | Horn, 1981 | M3 |
| 6 parameter 2nd order polynom | 8 Neighbors, Even Weighting Evans (Slope algorithms, 2015) | Evans, 1979 | M4 |
| 6 parameter 2nd order polynom | 8 Neighbors, Even Weighting Heerdegen (Slope algorithms, 2015) or 2nd Degree Polynomial Adjustment (García Rodríguez, Gimenez Suarez, 2010) | Heerdegen, Beran, 1982 | M5 |
| 6 parameter 2nd order polynom | Braunschweiger Relief Model (SAGA GIS, 2004) or 2nd Degree Polynomial Adjustment (García Rodríguez, Gimenez Suarez, 2010) | Bauer et al., 1985 | M6 |
| 9 parameter 2nd order polynom | Four Neighbors (Slope algorithms, 2015) or 2nd Degree Polynomial Adjustment (García Rodríguez, Gimenez Suarez, 2010) | Zevenbergen, Thorne, 1987 | M7 |

slope of the eight calculated slopes is then assigned to pixel Z_5 (Weih, Mattson, 2004):

$$s = \frac{\delta z}{d}$$

where:

- δz – the difference in value between the central pixel Z_5 and the neighbouring pixel Z_n
- d – distance between the central pixel Z_5 and the surrounding pixel Z_n , for pixels Z_2, Z_4, Z_6, Z_8 , this is the value of the side length of the pixel, but for Z_1, Z_3, Z_7, Z_9 , it is $\sqrt{2}$ (Dixon, Uddameri, 2016).

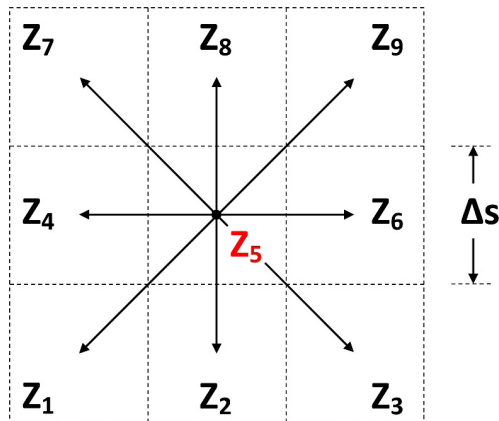


Figure 2. The slope of pixel Z_5 with respect to the 8 surrounding pixels Z_1 – Z_9 , for the Maximum Slope method (Travis et al., 1975). Black arrows indicate the directions of the slopes. Δs is the side length of the pixel (authors' own study).

The ideas of the so-called Deterministic 8 (O'Callaghan et al. 1984) method for calculating slope directions are the same as for maximum slopes (Travis et al., 1975). This method consists of calculating the largest slope with respect to 8 surrounding neighbours (Figure 3) (Dixon, Uddameri, 2016).

The measurement of the slope using the above method is not very accurate. A limitation of the Deterministic 8 method is the approximate direction of the runoff because the true direction of the runoff may be between the red arrow and the green arrow, e.g. the blue arrow (Figure 3). This limitation is due to the resolution of the DTM. The higher the resolution, the better the runoff direction will be reproduced relative to reality. An improved version of the method was proposed by Tarboton (Tarboton, 1997). It is called D-infinity (M2) and takes into account discretisation, which involves dividing the pixel area into smaller parts (triangles). This method takes the pixel with the largest slope and also two neighbouring pixels, whose values are used for more accurate calculations (Dixon, Uddameri, 2016) (Figure 4). In Figure 4, runoff is assigned to two pixels (p_1 and p_2 in yellow) based on the direction of ma-

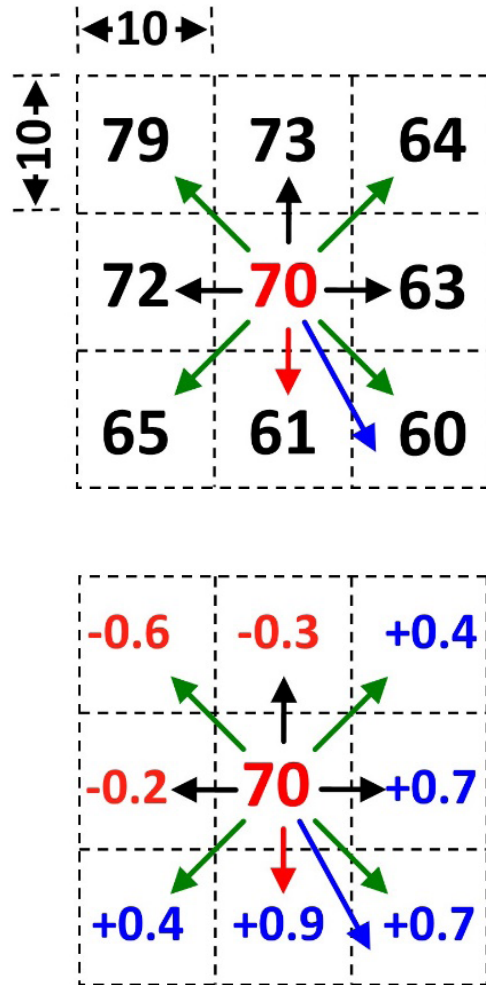


Figure 3. Example of calculating the greatest terrain slopes in relation to 8 surrounding neighbours. The upper part shows the pixel values, while the bottom part shows the slope gradient calculation values for the 8 surrounding neighbours. The black arrows represent the four nearest neighbours with pixel side length values. The green arrows represent the four nearest neighbours on the diagonal. The red arrow represents the direction of the largest slope. The blue arrow represents the other direction of slope, which is not included in the M1 method (authors' own study).

ximum slope, which are represented as 8 triangles. The proportions assigned to each pixel are determined by two coefficients (Smith et al., 2015):

$$p_1 = \frac{\alpha_2}{\alpha_1 + \alpha_2} \quad p_2 = \frac{\alpha_1}{\alpha_1 + \alpha_2}$$

where:

- α – direction in degrees or radians, measured from the side of the first triangle.

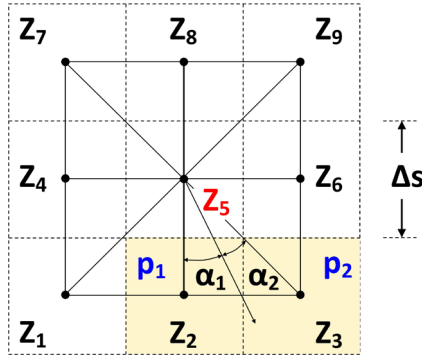


Figure 4. D-infinity method prepared on the basis of (Tarboton, 1997) (authors' own study).

Figure 4 shows the formulas for calculating the slope S:

$$\alpha_1 = \arctan\left(\frac{Z_2 - Z_3}{Z_5 - Z_2}\right)$$

$$S = \sqrt{\left(\frac{Z_2 - Z_3}{\Delta s}\right)^2 + \left(\frac{Z_5 - Z_2}{\Delta s}\right)^2}$$

(if α_2 does not fall within the triangle, the direction of the vector lies along the outermost edge),

where:

$Z_1, Z_2, Z_3, Z_4, Z_5, Z_6, Z_7, Z_8, Z_9$ – height values assigned to a pixel Δs – pixel size (Tarboton, 1997).

Figure 5 shows an example of the calculation of the slope direction α_2 and the slope S for Tarboton's method:

$$\alpha_1 = \arctan\left(\frac{61 - 60}{70 - 61}\right) = 6.3^\circ$$

$$S = \sqrt{\left(\frac{61 - 60}{10}\right)^2 + \left(\frac{70 - 61}{10}\right)^2} = 0.91$$

The result of the slope S gives a measure of the angle, which can be expressed in degrees, radians or grads.

In 1981 Horn proposed the Third-order Infinite Method for Calculating Slope (M3) (Horn, 1981; Weih et al., 2004), where the slope of the central pixel is obtained by solving the following equations based on the matrix in Figure 2:

$$\left[\frac{dz}{dx}\right] = \frac{(z_3 + 2z_6 + z_9) - (z_1 + 2z_4 + z_7)}{8\Delta}$$

$$\left[\frac{dz}{dy}\right] = \frac{(z_7 + 2z_8 + z_9) - (z_1 + 2z_2 + z_3)}{8\Delta}$$

$$S = \sqrt{\left[\frac{dz}{dx}\right]^2 + \left[\frac{dz}{dy}\right]^2}$$

where:

$Z_1, Z_2, Z_3, Z_4, Z_5, Z_6, Z_7, Z_8, Z_9$ – pixel value

S – tangent of the slope angle

Δs – pixel size.

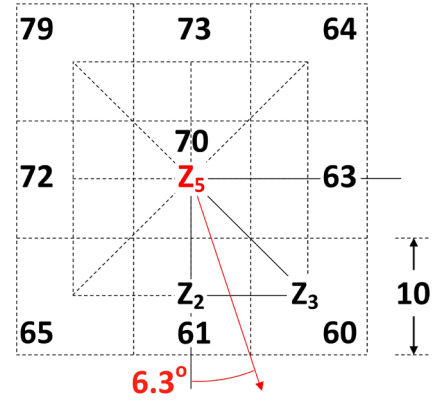


Figure 5. An example of the calculation of a slope using the D-infinity method (Tarboton, 1997) (authors' own study).

In the above case, pixels are assigned weights proportional to the inverse of the square of the distance from the central pixel (Drzewiecki et al., 1999).

The 8 Neighbors, Even Weighting Heerdegen (M5) method (Heerdegen, Beran, 1982; Garcia Rodriguez, Gimenez Suarez, 2010) consists of two stages. In the first stage, equations were obtained from the pixel matrix shown in Figure 2:

$$V_1 = Z_1 + Z_3 + Z_4 + Z_6 + Z_7 + Z_9$$

$$V_2 = Z_1 + Z_2 + Z_3 + Z_7 + Z_8 + Z_9$$

$$V_3 = Z_1 - Z_3 - Z_7 + Z_9$$

$$V_4 = -Z_1 + Z_3 - Z_4 + Z_6 - Z_7 + Z_9$$

$$V_5 = -Z_1 - Z_2 - Z_3 + Z_7 + Z_8 + Z_9$$

from which the following coefficients were derived:

$$a = \frac{0.3 \cdot v_1 - 0.2 \cdot v_2}{G^2}$$

$$b = \frac{0.3 \cdot v_2 - 0.2 \cdot v_1}{G^2}$$

$$c = \frac{v_3}{4 \cdot G^2}$$

$$d = \frac{v_4}{6 \cdot G}$$

$$e = \frac{v_5}{6 \cdot G}$$

where G is the pixel size. In the next step, the four parameters are calculated using formulas:

$$[\text{slope vector } (^\circ)] = 180 - \tan^{-1}\left(\frac{-e}{-d}\right) - 90\left(\frac{-d}{|d|}\right)$$

$$[\text{gradient } (mm^{-1})] = (d^2 + e^2)^{0.5}$$

$$[\text{plan curvature } (m^{-1})] = \frac{e(c \cdot d - 2 \cdot a \cdot e)}{(d^2 + e^2)^{1.5}}$$

$$[\text{slope curvature } (m^{-1})] = \frac{2(a \cdot d^2 + b \cdot e^2 + c \cdot d \cdot e)}{(d^2 + e^2) \cdot (1.0 + d^2 + e^2)^{1.5}}$$

The next three methods analysed for calculating terrain slopes: 2nd Degree Polynomial Adjustment (M7) (Zevenbergen, Thorne, 1987; Garcia Rodriguez, Gimenez Suarez, 2010), 8 Neighbors, Even Weighting Evans (M4) (Evans, 1979; Slope algorithms, 2015) and Braunschweiger Relief Model (M6) (Bauer et al., 1985; Garcia Rodriguez, Gimenez Suarez, 2010) consist of polynomial equations. However, they differ in the number of parameters. For the 2nd Degree Polynomial Adjustment (M7) method (Zevenbergen, Thorne, 1987; Garcia Rodriguez, Gimenez Suarez, 2010), all nine pixels with specific values, distributed in a 3×3 matrix, are used to calculate the A-I coefficients, which in a further step are used to calculate the slope value at the centre pixel of the central matrix (Drzewiecki et al., 1999). The polynomial has the form:

$$Z = Ax^2y^2 + Bx^2y + Cxy^2 + Dx^2 + Ey^2 + Fxy + Gx + Hy + I$$

where:

$$A = \frac{\left(\frac{Z_1 + Z_3 + Z_7 + Z_9}{4} - \frac{Z_2 + Z_4 + Z_6 + Z_8}{2} + Z_5\right)}{L^4}$$

$$B = \frac{\left(\frac{Z_1 + Z_3 - Z_7 - Z_9}{4} - \frac{Z_2 - Z_8}{2}\right)}{L^3}$$

$$C = \frac{\left(\frac{-Z_1 + Z_3 - Z_7 + Z_9}{4} - \frac{Z_4 - Z_6}{2}\right)}{L^3}$$

$$D = \frac{\left(\frac{Z_4 + Z_6}{2} - Z_5\right)}{L^2}$$

$$E = \frac{\left(\frac{Z_2 + Z_8}{2} - Z_5\right)}{L^2}$$

$$F = \frac{-Z_1 + Z_3 + Z_7 - Z_9}{4 - L^2}$$

$$G = \frac{-Z_4 + Z_6}{2 \cdot L}$$

$$H = \frac{Z_2 + Z_8}{2 \cdot L}$$

$$I = Z_5$$

L – pixel size

$Z_1, Z_2, Z_3, Z_4, Z_5, Z_6, Z_7, Z_8, Z_9$ – pixel values.

For method 8 Neighbors, Even Weighting Evans (M4) (1979, Evans; Slope algorithms, 2015) the polynomial is of the form:

$$Z = Ax^2 + By^2 + Cxy + Dx + Ey + F$$

where:

$$A = \frac{(Z_1 + Z_3 + Z_4 + Z_6 + Z_7 + Z_9) - 2 \cdot (Z_2 + Z_5 + Z_8)}{6 \cdot L^2}$$

$$B = \frac{(Z_1 + Z_2 + Z_3 + Z_7 + Z_8 + Z_9) - 2 \cdot (Z_4 + Z_5 + Z_6)}{6 \cdot L^2}$$

$$C = \frac{Z_3 + Z_7 - Z_1 - Z_9}{4 \cdot L^2}$$

$$D = \frac{Z_3 + Z_6 + Z_9 - Z_1 - Z_4 - Z_7}{6 \cdot L^2}$$

$$E = \frac{Z_1 + Z_2 + Z_3 - Z_7 - Z_8 - Z_9}{6 \cdot L^2}$$

$$F = Z_5$$

L – pixel size

$Z_1, Z_2, Z_3, Z_4, Z_5, Z_6, Z_7, Z_8, Z_9$ – pixel values.

However, the polynomial in the method 2nd Degree Polynomial Adjustment (M6) (Bauer i in., 1985; Garcia Rodriguez, Gimenez Suarez, 2010) takes the form:

$$Z = Ax^2 + By^2 + Cxy + Dx + Ey + F$$

where:

$$A = \frac{(Z_1 + Z_3 + Z_4 + Z_6 + Z_7 + Z_9) - 2 \cdot (Z_2 + Z_5 + Z_8)}{L^2}$$

$$B = \frac{(Z_1 + Z_2 + Z_3 + Z_7 + Z_8 + Z_9) - 2 \cdot (Z_4 + Z_5 + Z_6)}{L^2}$$

$$C = \frac{Z_9 + Z_1 - Z_8}{4 \cdot L^2}$$

$$D = \frac{(Z_3 - Z_1) + (Z_6 - Z_4) + (Z_9 - Z_7)}{6 \cdot L^2}$$

$$E = (Z_7 - Z_1) + (Z_8 - Z_2) + (Z_9 - Z_3)$$

$$F = Z_5$$

L – pixel size

$Z_1, Z_2, Z_3, Z_4, Z_5, Z_6, Z_7, Z_8, Z_9$ – pixel values.

Based on the above polynomial, the value of the slope originating at the centre of the central pixel is calculated (Drzewiecki et al., 1999).

Statistical analysis of the results of different methods for determining terrain slopes from DTMs with different resolutions

The datasets (ARC/INFO ASCII GRID) used in this publication come from the Main Center for Geodesic and Cartographic Documentation (CODGiK, 2013). They are text files saved as a matrix, containing the height value of points in a regular grid with a mesh of 1 m. The dataset was obtained via interpolation from the point cloud from airborne laser scanning (LIDAR) by CODGiK centre and

is used in Poland as a standard DTM reference. The mean error in height is within 0.2 m.

The data are split into sheets in files by headings for the 1992 rectangular planar coordinate system (EPSG:2180), at a scale of 1:5000 (CODGiK, 2013). Quantum GIS 2.18.5 and SAGA GIS 4.0.1 software were used to process the data. The datasets were loaded into SAGA GIS in the form of files (ARC/INFO ASCII GRID), representing the individual DTM sheets according to the emblems (1992 layout) and combined using the mosaicking tool (Mosaicking). All DTM sheets are in the same coordinate system and format. Then, for a unified raster with a resolution of 1 m, a generalisation of the DTM was carried out using the 'resampling' tool (Resampling). Resampling was performed using nearest neighbour interpolation (Rukundo, Cao, 2012; Urbański, 2012). Generalised raster resolutions of 5, 10, 30 and 90 meters were produced. In the next step, for individual resolutions of 1, 5, 10, 30 and 90 meters, the catchment boundary of the Bystra River was delineated using the 'Basic Terrain Analysis' tool where the catchment area boundary and the river channel network were created.

In the next step, for the specified resolutions of 1, 5, 10, 30, 90 meters, rasters with slopes were created for 7 slope calculation methods in SAGA GIS software: M1–M7 using the 'slope, aspect, curvature' tool. The unit of slopes

for the obtained rasters is degrees. The obtained rasters were cut with the boundary of the catchment area using the 'Clip Grid with Polygon' tool. This resulted in identical rasters in terms of pixel counts, which will serve for comparison purposes (Figure 7). The rasters obtained for the M1 method, for pixel sizes 1, 5, 10, 30, 90 contained empty pixels. In the Quantum GIS software, these were filled in using the 'Fill Nodata' tool. Histograms showing the number of pixels were also generated, showing the corresponding slope in degrees (Figure 8).

After receiving the finished rasters with slope gradients in SAGA GIS, the following terrain slope statistics were generated for each raster using the 'Save Grid Statistics to Table' tool: number of pixels in the raster, pixel size, arithmetic mean, minimum value, maximum value, range of values, variance, standard deviation (Table 2).

From the analysis of Table 2, it can be concluded that for the processed rasters, the three methods for calculating slopes M4, M5 and M6 give identical results, while M3 has similar results to the above methods. Methods M1, M2 and M7 produce a larger range of slope angles compared to methods M3, M4, M5, M6. The maximum values of the slopes are also higher. The largest range and maximum value of slope gradients occur for methods representing a resolution of 1 m pixel size. In contrast, the smallest

Table 2. Comparison of slope calculation methods in relation to pixel size (authors' own study).

| Method | Number of data pixel | Pixel size [m] | Arithmetic mean [°] | Minimum [°] | Maximum [°] | Range [°] | Variance [°] | Standard deviation [°] |
|--------|----------------------|----------------|---------------------|-------------|-------------|-----------|--------------|------------------------|
| M1 | 309816175 | 1 | 5.0 | 0.0 | 83.6 | 83.6 | 47.6 | 6.9 |
| M2 | 309791387 | 1 | 5.2 | 0.4 | 83.6 | 83.2 | 48.5 | 7.0 |
| M3 | 309816175 | 1 | 4.5 | 0.0 | 81.3 | 81.3 | 46.2 | 6.8 |
| M4–M6 | 309816175 | 1 | 4.5 | 0.0 | 81.2 | 81.2 | 45.9 | 6.8 |
| M7 | 309816175 | 1 | 4.7 | 0.0 | 81.6 | 81.6 | 47.0 | 6.9 |
| M1 | 12392647 | 5 | 4.0 | 0.0 | 73.0 | 73.0 | 38.0 | 6.2 |
| M2 | 12392547 | 5 | 4.1 | 0.0 | 73.0 | 73.0 | 39.2 | 6.3 |
| M3 | 12392647 | 5 | 3.7 | 0.0 | 66.0 | 66.0 | 30.8 | 5.5 |
| M4–M6 | 12392647 | 5 | 3.7 | 0.0 | 65.8 | 65.8 | 30.2 | 5.5 |
| M7 | 12392647 | 5 | 3.8 | 0.0 | 70.6 | 70.6 | 33.4 | 5.8 |
| M1 | 3101700 | 10 | 3.7 | 0.0 | 63.5 | 63.5 | 31.6 | 5.6 |
| M2 | 3101699 | 10 | 3.9 | 0.0 | 63.8 | 63.8 | 32.7 | 5.7 |
| M3 | 3101700 | 10 | 3.4 | 0.0 | 52.9 | 52.9 | 22.3 | 4.7 |
| M4–M6 | 3101700 | 10 | 3.4 | 0.0 | 52.0 | 52.0 | 21.7 | 4.7 |
| M7 | 3101700 | 10 | 3.5 | 0.0 | 59.4 | 59.4 | 25.3 | 5.0 |
| M1 | 326778 | 30 | 3.4 | 0.0 | 42.0 | 42.0 | 20.8 | 4.6 |
| M2 | 326778 | 30 | 3.5 | 0.0 | 42.0 | 42.0 | 21.7 | 4.7 |
| M3 | 326778 | 30 | 2.8 | 0.0 | 31.7 | 31.7 | 11.9 | 3.4 |
| M4–M6 | 326778 | 30 | 2.8 | 0.0 | 31.4 | 31.4 | 11.4 | 3.4 |
| M7 | 326778 | 30 | 3.0 | 0.0 | 33.6 | 33.6 | 14.4 | 3.8 |
| M1 | 35770 | 90 | 2.6 | 0.0 | 27.9 | 27.9 | 9.1 | 3.0 |
| M2 | 35769 | 90 | 2.7 | 0.0 | 27.9 | 27.9 | 9.4 | 3.1 |
| M3 | 35770 | 90 | 1.9 | 0.0 | 18.7 | 18.7 | 4.0 | 2.0 |
| M4–M6 | 35770 | 90 | 1.9 | 0.0 | 18.4 | 18.3 | 3.8 | 1.9 |
| M7 | 35770 | 90 | 2.1 | 0.0 | 20.3 | 20.3 | 5.3 | 2.3 |

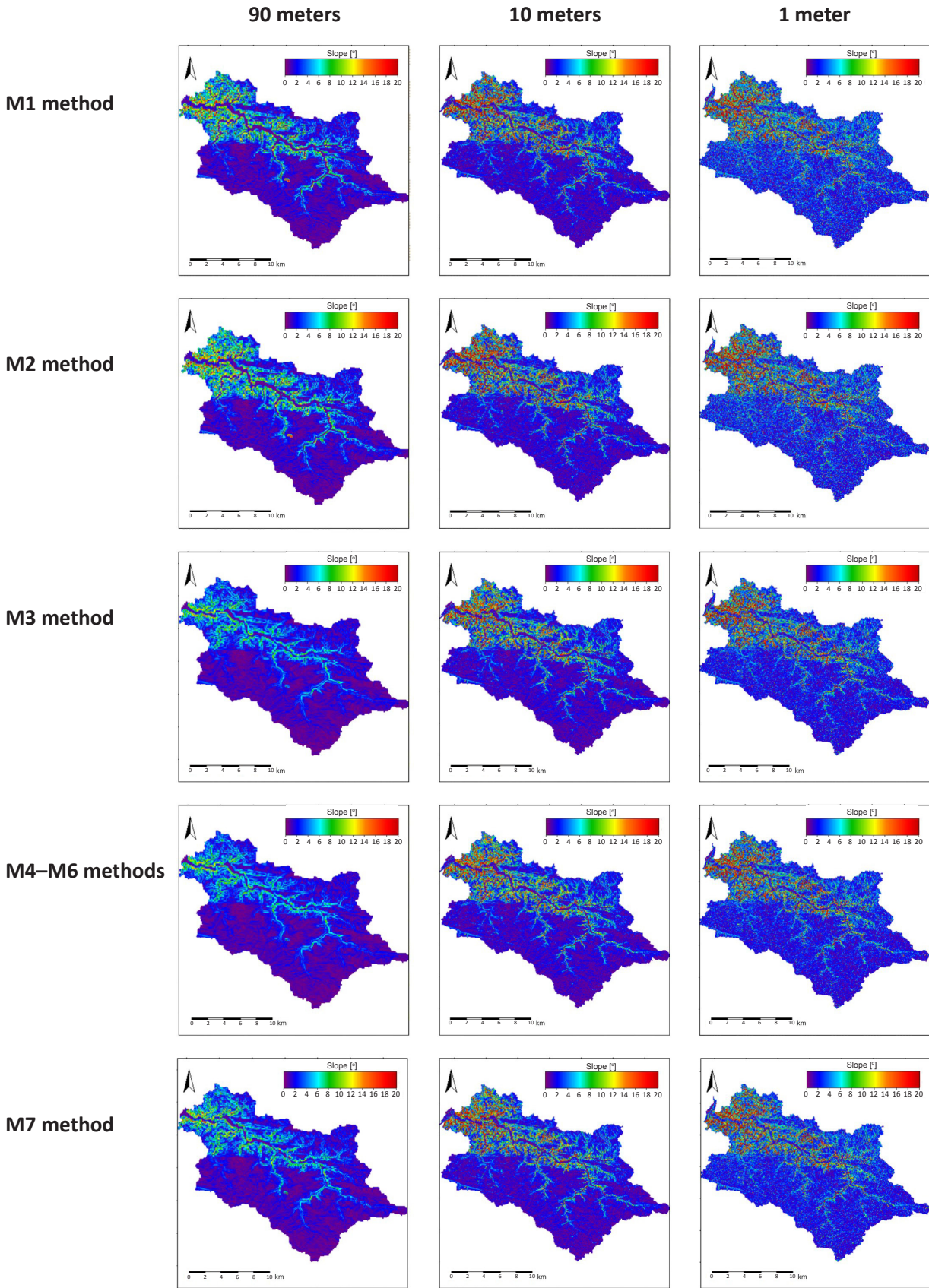


Figure 7. Maps with calculated slopes for different algorithms at 90, 10, 1 meter for M1–M7 method (authors' own study).

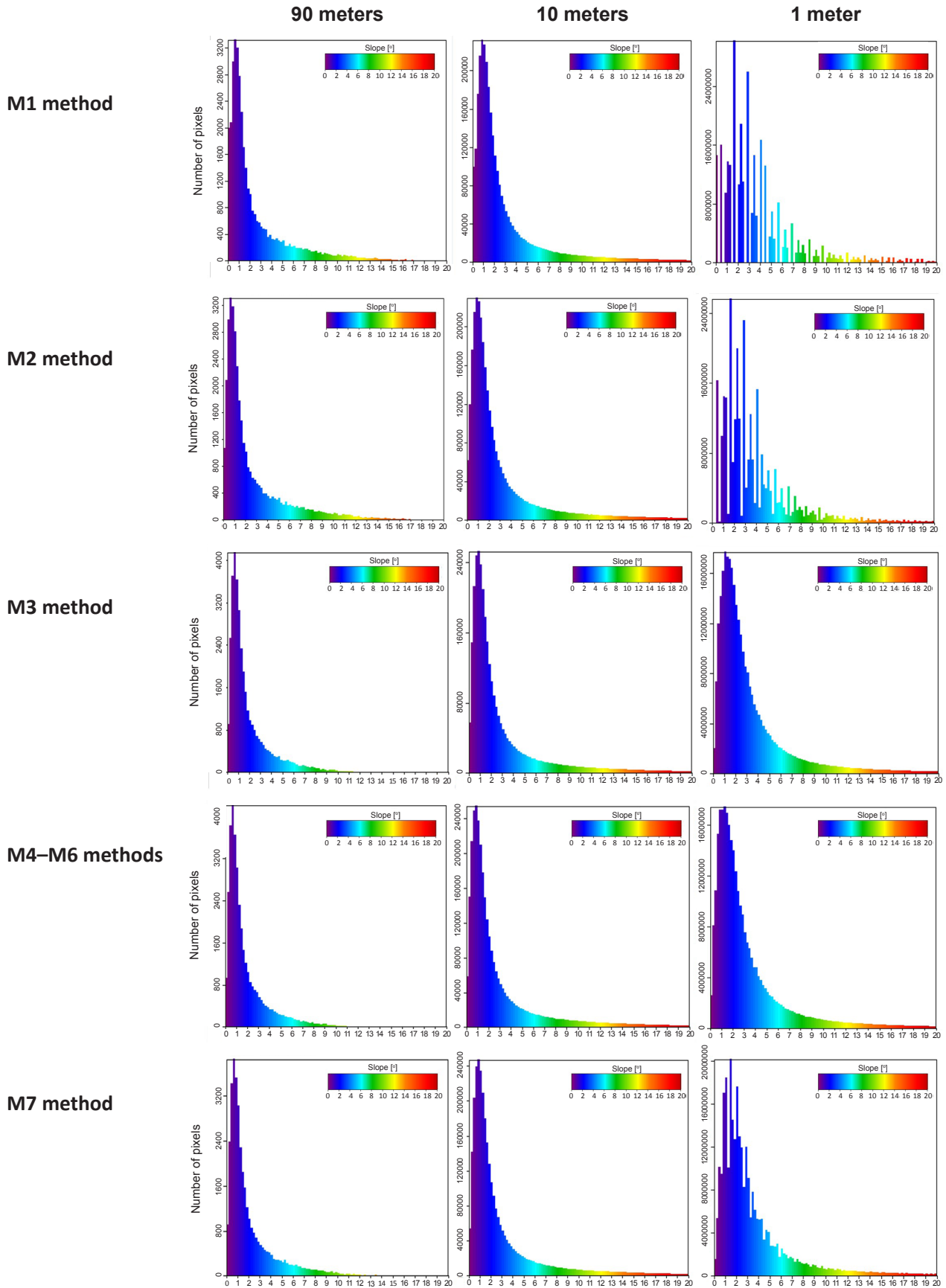


Figure 8. The histograms show the number of pixels for angle value at 90, 10, 1 meter for M1–M7 method (authors’ own study).

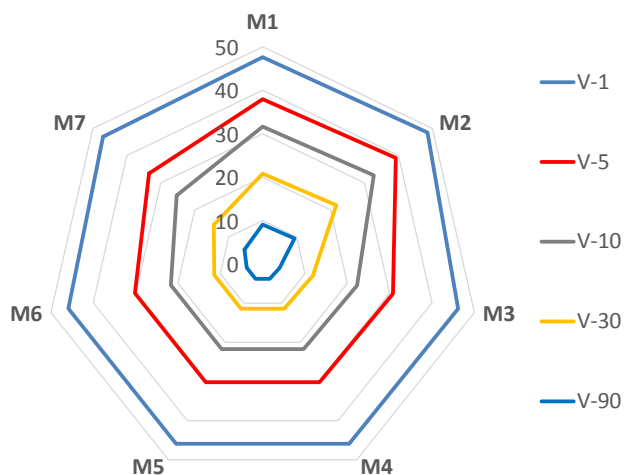


Figure 9. Comparison of variance for slope calculation methods with respect to pixel size (authors' own study).

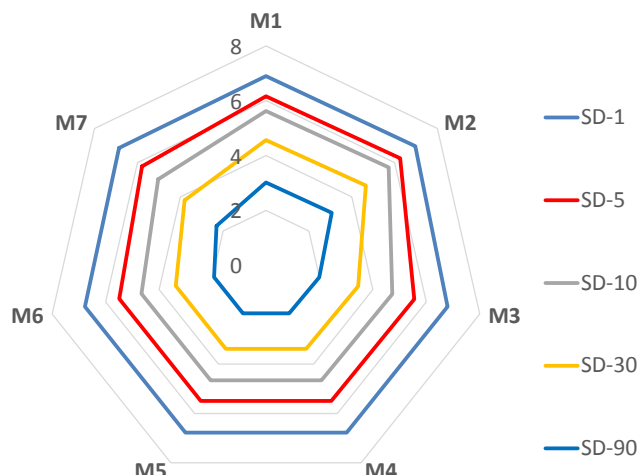


Figure 10. Comparison of standard deviation for slope calculation methods with respect to pixel size (authors' own study).

ranges and slope values are presented by methods representing a resolution with a pixel size of 90 m.

The resulting statistics for the falls were also compared with each other in terms of variance and standard deviation (Figure 9, Figure 10).

The figures and tables of the standard deviation as well as the variance (Figure 9, Figure 10) show the general relationship of the reduction in variance and standard deviation as the pixel size increases. For a pixel size of 1, the variance and standard deviation for each method used gives approximate results. For a pixel size of 90, the variance and standard deviation vary according to the method used.

Analysis of the number of pixels within a given range of terrain slopes for different resolutions

In the further analysis of the methods for calculating slopes, the raster pixels corresponding to each slope were classified into one of the corresponding ranges (Table 3). The slope ranges are derived from the PWER (Potential Water Erosion Indicator) and AWER (Actual Water Erosion Indicator) indicators for soil erosion risk, which are the standard for visualising relief in Poland (Wawer et al., 2006).

Table 3. Slopes in compartments (Wawer et al., 2006).

| | | | |
|--------|---|--------|---------|
| 0.00° | – | 2.99° | range 0 |
| 3.00° | – | 5.99° | range 1 |
| 6.00° | – | 9.99° | range 2 |
| 10.00° | – | 14.99° | range 3 |
| ≥15° | | | range 4 |

The above assignment of each pixel to an appropriate compartment in further analysis gives the possibility to see what number of pixels corresponds to a given terrain slope compartment and how it varies with pixel size. The assignment of pixels to individual compartments was done in Quantum GIS software using the r.reclass process, which is derived from GRASS GIS software. Once the pixels were assigned to each interval, a statistical report of the number of pixels in the interval was made using the r.report process. This number of pixels was then recalculated in terms of the area occupied in hectares (Table 4).

A comparison was made of the percentage of area in hectares of a given fall interval in relation to the total area for a given resolution (Figures 11-15).

For 1 m resolution, the majority of pixels fall into the 0.00°–2.99° and 3.00°–5.99° intervals. For resolutions of 5, 10, 30 meters the percentage distribution of pixels in the slope intervals is similar for all methods. For a pixel size of 90 m, the dominant slope interval is the 0.00°–2.99° interval.

In the next step, the dependence of the resolution of 1, 5, 10, 30, 90 meters on the number of pixels in the interval was compared.

Analysing the above figures of the percentage share of a given interval for resolutions of 1, 5, 10, 30 and 90 meters for the 7 methods calculating terrain slope (Figures 16-20), it can be seen that for methods M3, M4, M5, M6 the differences in the percentage share of a given interval for resolutions of 1, 5, 10, 30 and 90 meters are the smallest. Slightly larger differences are shown in the figure for methods M1, M2.

Table 4. Comparison of areas in individual slope ranges for slope calculation methods (authors' own study).

| Method | 0.00°–2.99° | 3.00°–5.99° | 6.00°–9.99° | 10.00°–14.99° | ≥15° | Total area [ha] | Pixel size [m] |
|--------|-------------|-------------|-------------|---------------|------|-----------------|----------------|
| M1 | 13812 | 9742 | 3836 | 1520 | 2071 | 30982 | 1 |
| M2 | 12805 | 10593 | 3916 | 1548 | 2118 | 30979 | 1 |
| M3 | 16656 | 8257 | 2798 | 1289 | 1982 | 30982 | 1 |
| M4–M6 | 16848 | 8106 | 2765 | 1285 | 1978 | 30982 | 1 |
| M7 | 15655 | 8975 | 3011 | 1331 | 2009 | 30982 | 1 |
| M1 | 19202 | 6306 | 2355 | 1260 | 1859 | 30982 | 5 |
| M2 | 18897 | 6460 | 2417 | 1291 | 1918 | 30981 | 5 |
| M3 | 19964 | 5700 | 2309 | 1311 | 1698 | 30982 | 5 |
| M4–M6 | 19995 | 5677 | 2309 | 1317 | 1684 | 30982 | 5 |
| M7 | 19714 | 5891 | 2323 | 1291 | 1763 | 30982 | 5 |
| M1 | 19969 | 5656 | 2301 | 1323 | 1768 | 31017 | 10 |
| M2 | 19665 | 5800 | 2361 | 1355 | 1836 | 31017 | 10 |
| M3 | 20499 | 5372 | 2341 | 1408 | 1396 | 31017 | 10 |
| M4–M6 | 20535 | 5357 | 2345 | 1415 | 1365 | 31017 | 10 |
| M7 | 20288 | 5502 | 2325 | 1367 | 1535 | 31017 | 10 |
| M1 | 19362 | 4845 | 2371 | 1531 | 1301 | 29410 | 30 |
| M2 | 19015 | 4979 | 2440 | 1593 | 1382 | 29410 | 30 |
| M3 | 20060 | 4948 | 2559 | 1322 | 521 | 29410 | 30 |
| M4–M6 | 20125 | 4958 | 2562 | 1294 | 472 | 29410 | 30 |
| M7 | 19837 | 4930 | 2469 | 1402 | 772 | 29410 | 30 |
| M1 | 20188 | 4811 | 2611 | 1140 | 222 | 28974 | 90 |
| M2 | 19706 | 5053 | 2756 | 1213 | 244 | 28973 | 90 |
| M3 | 22029 | 4933 | 1722 | 273 | 17 | 28974 | 90 |
| M4–M6 | 22188 | 4897 | 1637 | 239 | 13 | 28974 | 90 |
| M7 | 21321 | 4986 | 2115 | 504 | 49 | 28974 | 90 |

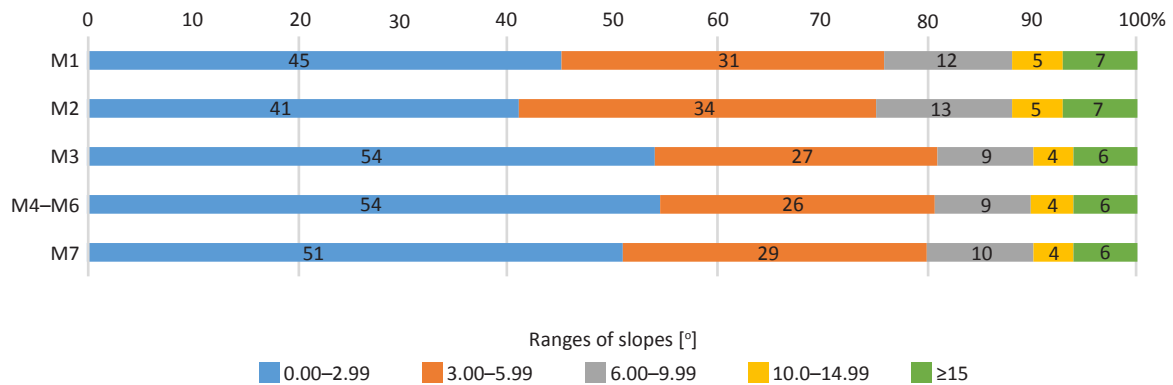


Figure 11. Percentage of pixels for 1 meter resolution for individual methods of calculating the terrain slope (authors' own study).

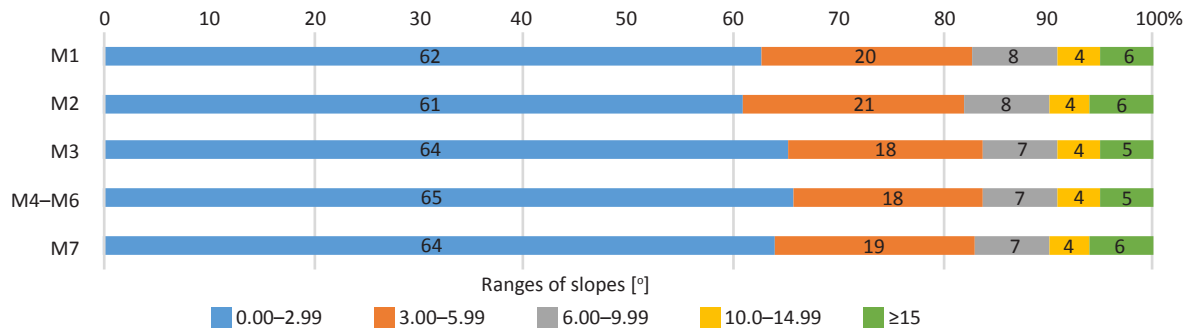


Figure 12. Percentage of pixels for 5 meter resolution for individual methods of calculating the terrain slope (authors' own study).

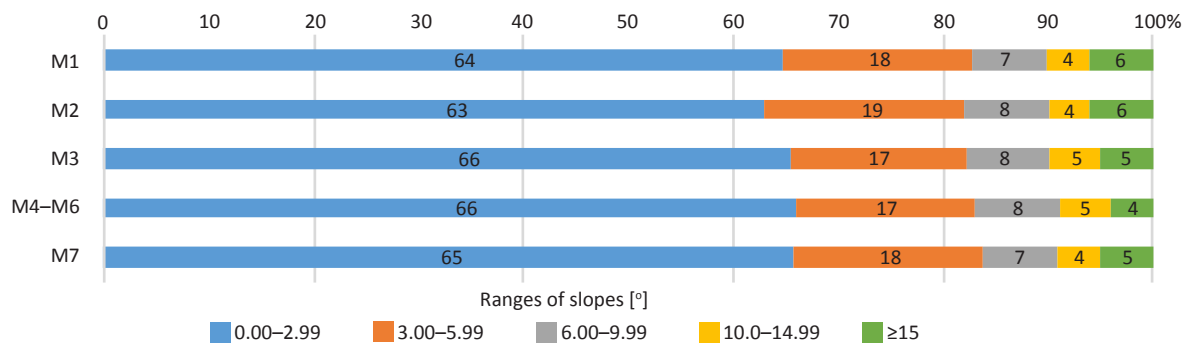


Figure 13. Percentage of pixels for 10 meter resolution for individual methods of calculating the terrain slope (authors' own study).

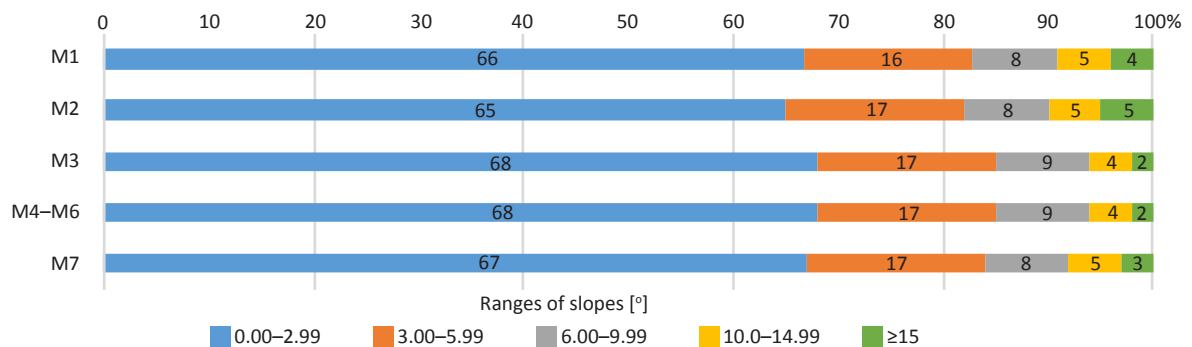


Figure 14. Percentage of pixels for 30 meter resolution for individual methods of calculating the terrain slope (authors' own study).

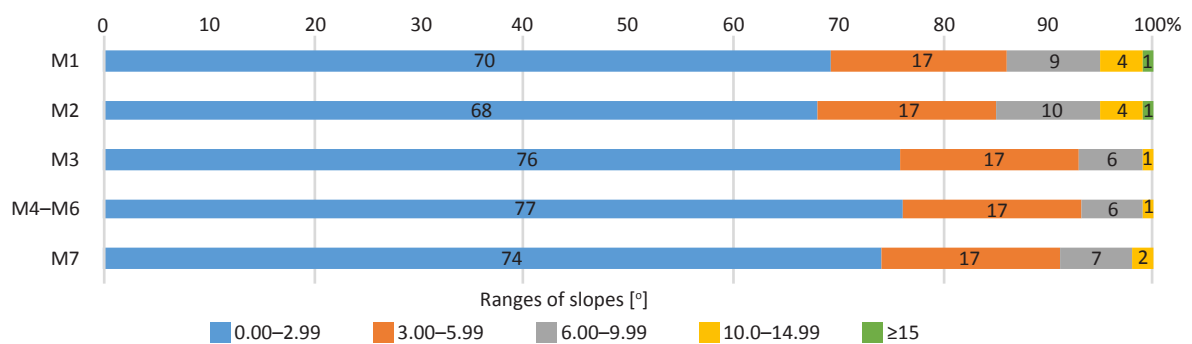


Figure 15. Percentage of pixels for 90 meter resolution for individual methods of calculating the terrain slope (authors' own study).

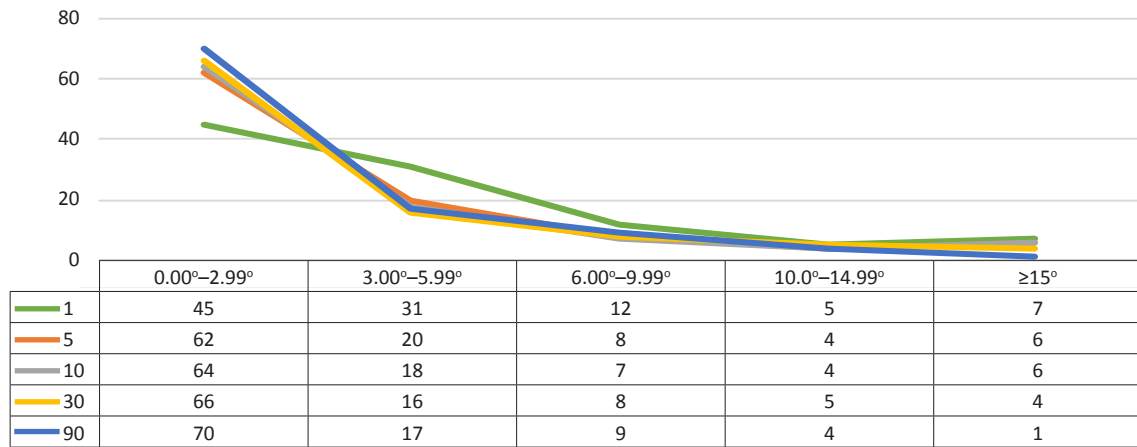


Figure 16. Percentage share of pixels in ranges of slopes for the M1 method (authors' own study).

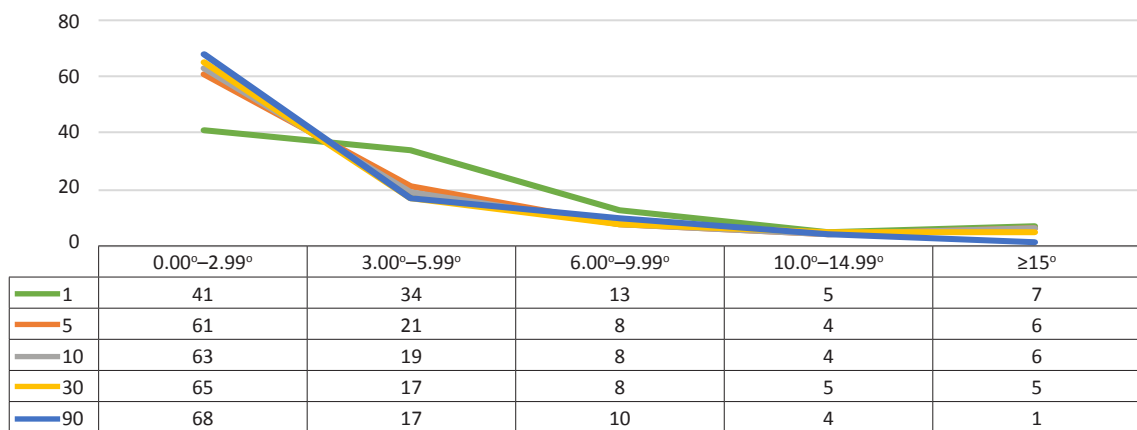


Figure 17. Percentage share of pixels in ranges of slopes for the M2 method (authors' own study).

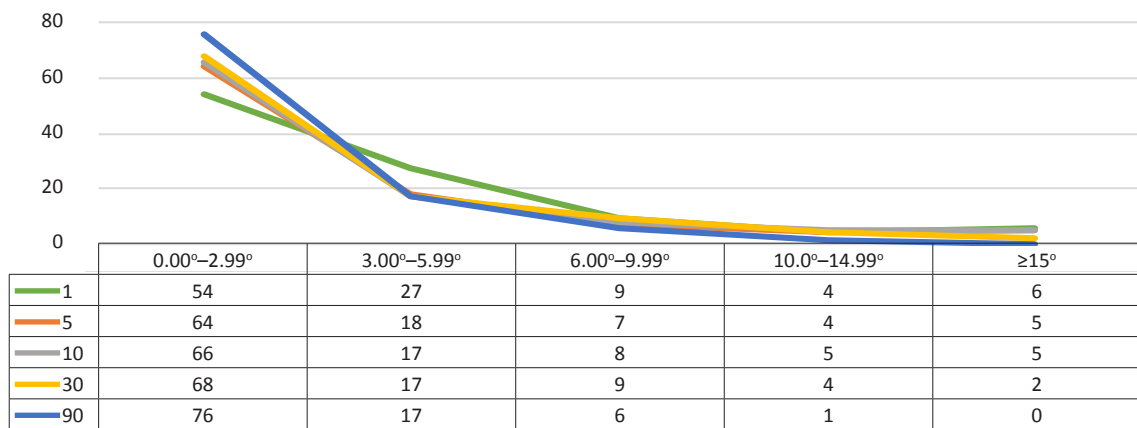


Figure 18. Percentage share of pixels in ranges of slopes for the M3 method (authors' own study).

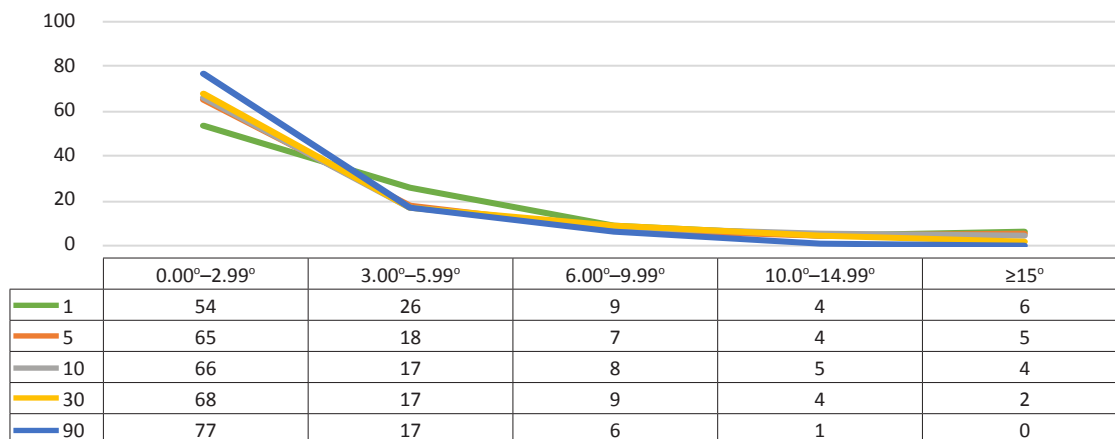


Figure 19. Percentage share of pixels in ranges of slopes for the M4–M6 method (authors' own study).

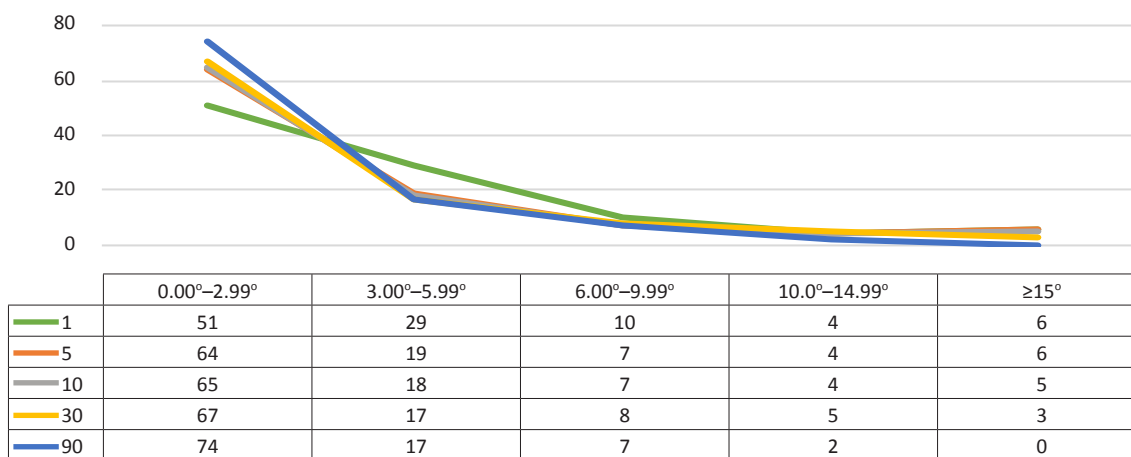


Figure 20. Percentage share of pixels in ranges of slopes for the M7 method (authors' own study).

Comparison of calculated slopes with field measurements

The next chapter compares the topographic profile (Figure 21) located in the vicinity of Esterka Castle in Bochońnica, obtained by geodetic survey, with the topographic profiles obtained in Quantum GIS software for resolutions of 1, 5, 10, 30 and 90 meters.

The geodetic, tachymetric measurement at 90 points resulted in a topographic profile, the course of which is shown on the orthophoto (Figure 21). Below the orthophotos, the topographic profiles for the different DTM resolutions are juxtaposed with the profile generated after the geodetic measurement. The height difference between the highest point and the lowest point in the topographic profile for both the geodetic measurement and the one generated in the Quantum GIS software is approximately

74 meters. Between the profile measured geodetically and the one generated in the Quantum GIS program, similarities can be seen in the slopes of the terrain. The topographic profiles generated for a resolution of 1, 5 and 10 meters do not differ and are similar to the geodetic measurement. A closer analysis of the topographic profile with a resolution of 1 m generated in Quantum GIS with the geodetic measurement (Figure 21) shows differences of a few meters over certain sections, e.g. 200 to 250 meters, 320 to 350 meters. In contrast, a topographic profile with a resolution of 30 m shows a greater variation in the terrain than is actually the case. For a large pixel size of 90 m, it is not possible to assess the relief and slope accurately.

In order to more accurately verify the topographic profile with a resolution of 1 m, a more accurate geodetic survey was taken every 1.5 meters at 20 points along the initial section of the topographic profile (Figure 22).

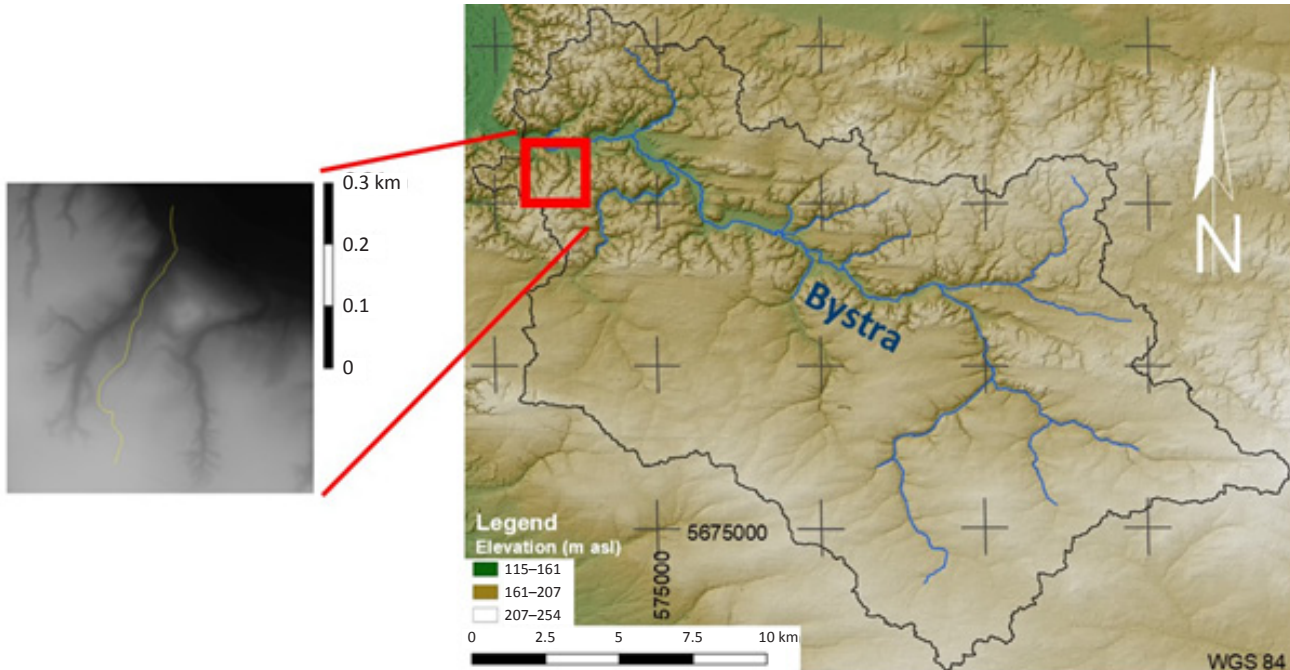


Figure 21. The measured topographic profile of the basin of the river Bystra (authors' own study).

The difference between the 1 m resolution profile generated in the Quantum GIS software and the geodetic measurement ranges from a few to several centimeters (Figure 24). The approximate height difference between the highest and lowest measured points in the field, over a distance of 33.2 meters, was 2.4 meters and the calculated slope was 4.1 degrees. In the next step, the calculated slope of 4.1 degrees was compared with the slopes calculated in the Quantum GIS software for resolutions of 5, 10, 30 and 90 meters.

The slopes calculated for a resolution of 90 meters for methods M3, M4, M5, M6, M7 (Figure 25) have values approximating the slope calculated from the figure (Figure 24).

For methods M1 and M2, the slope values are higher. For a resolution of 30 m, all methods of calculating the slopes (Figure 26) give slope gradient values similar to the one calculated in the figure (Figure 24).

For a resolution of 10 meters, all methods of calculating slopes give approximate values (Figure 27). For a resolution of 5 meters, the results are similar (Figure 28).

DISCUSSION

The calculation of terrain slopes in a GIS environment is usually based on the use of a single selected method. In SAGA GIS it is possible to use a number of different methods to calculate slopes. Methods: Maximum Slope (M1) and D-infinity (M2), and the Third-order Infinite Method

for Calculating Slope (M3), have some limitations due to the inability to calculate all types of curvature. The above three methods focus on flow routing logic, operate on a local scale and have particular limitations as they calculate slope in one direction from one pixel to another (Singer, 2015). The remaining methods are able to calculate all types of curvature. The results of slope calculations for the first three methods (M1, M2, M3) are compared to the other methods: 8 Neighbors, Even Weighting Evans; 8 Neighbors, Even Weighting Heerdegen; Braunschweiger Relief Model (M4, M5, M6), 2nd Degree Polynomial Adjustment (M7). For the maximum slope (M1) and maximum triangle slope (M2) methods for 1 m resolution, the percentage of pixels in the 0.00° – 2.99° interval was 44.6%, 41.3% respectively. For the other methods, the values range from 50.5% to 54.4%. For the 3.00° – 5.99° interval for methods M1 and M2 the pixel share is 31.4% and 34.2% respectively. For the other methods, however, the values range from 26.2% to 29%. For the interval 6.00° – 9.99° for methods M1 and M2, the pixel share is 12.4% and 12.6% respectively. For the other methods, however, the values range from 8.9% to 9.7%.

Methods M3, M4, M5 have almost identical slope calculation results. Method M7 has similar slope calculation results for different resolutions compared to methods M4, M5, M6. For the 1 m resolution of methods M3, M4, M5 for the 0.00° – 2.99° interval, the pixel share is 54.4%, while for the 3.00° – 5.99° interval, the pixel share is 26.2%. Compared to method M7, for the 0.00° – 2.99° interval the pixel

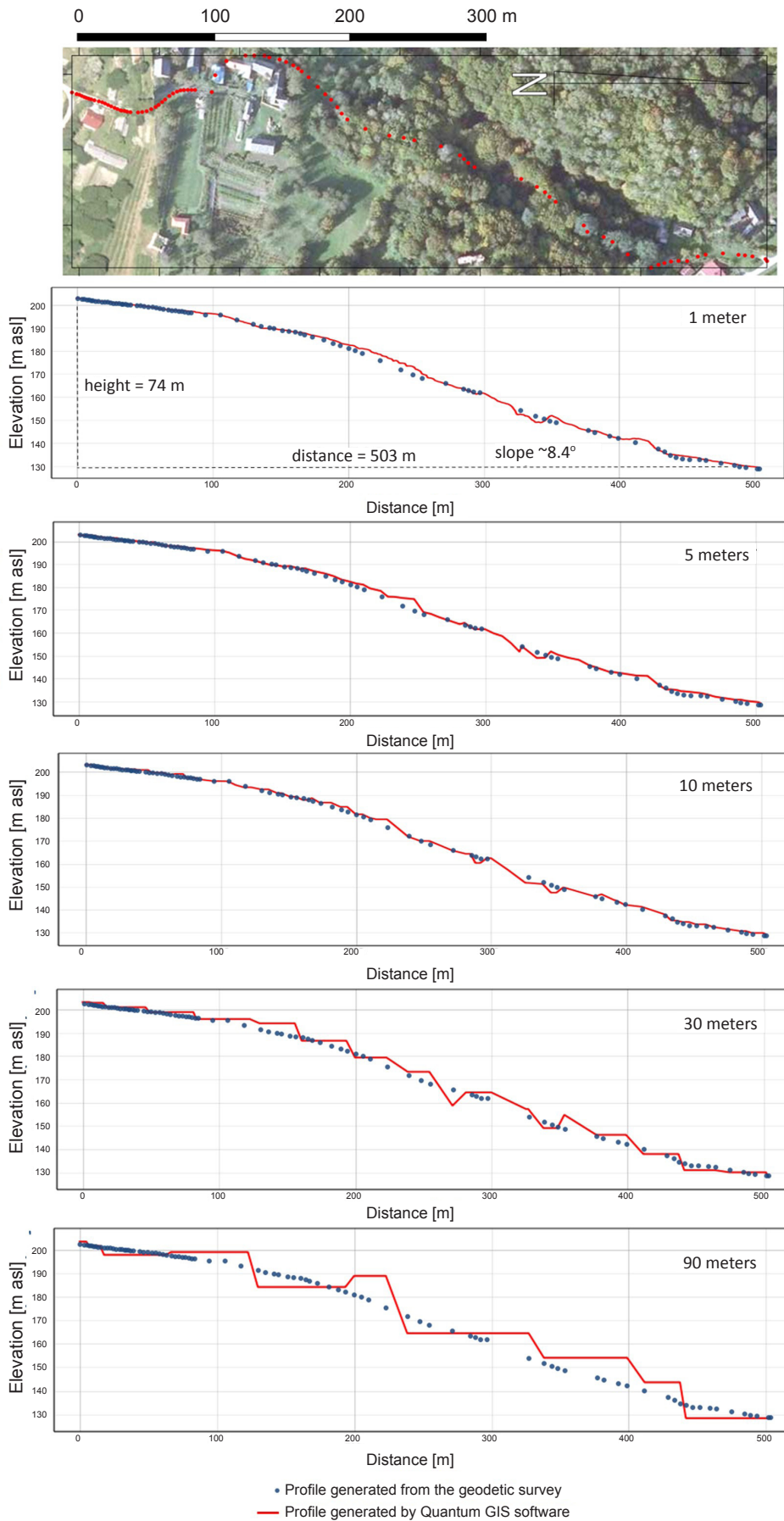


Figure 22. Comparison of profile of slopes for spatial resolution 1, 5, 10, 30 and 90 meters with survey data collection, which was made by a tachymeter (authors' own study).

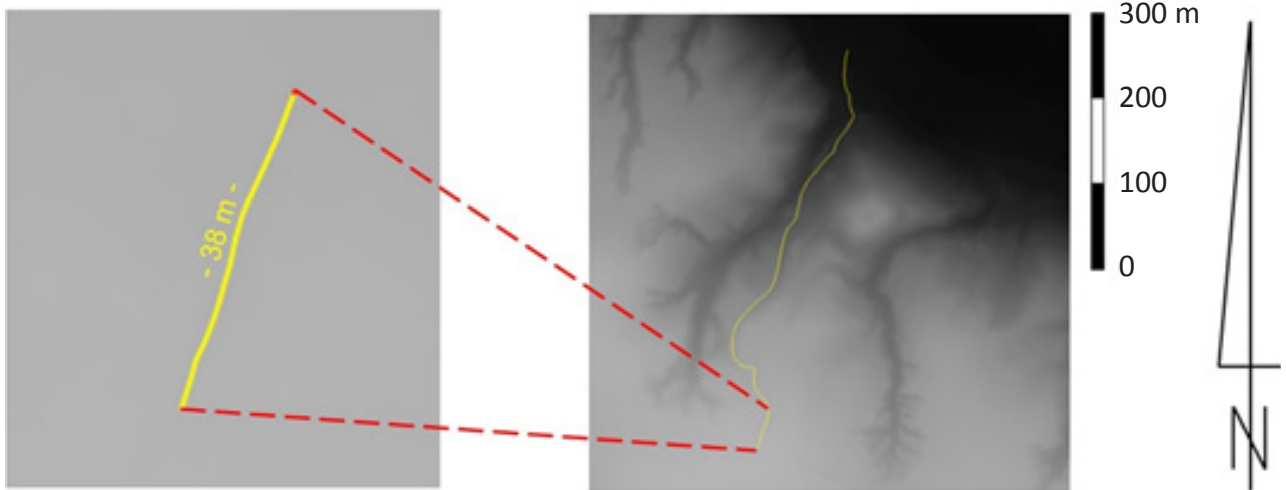


Figure 23. The measured topographic profile of the basin of the river Bystra (authors' own study).

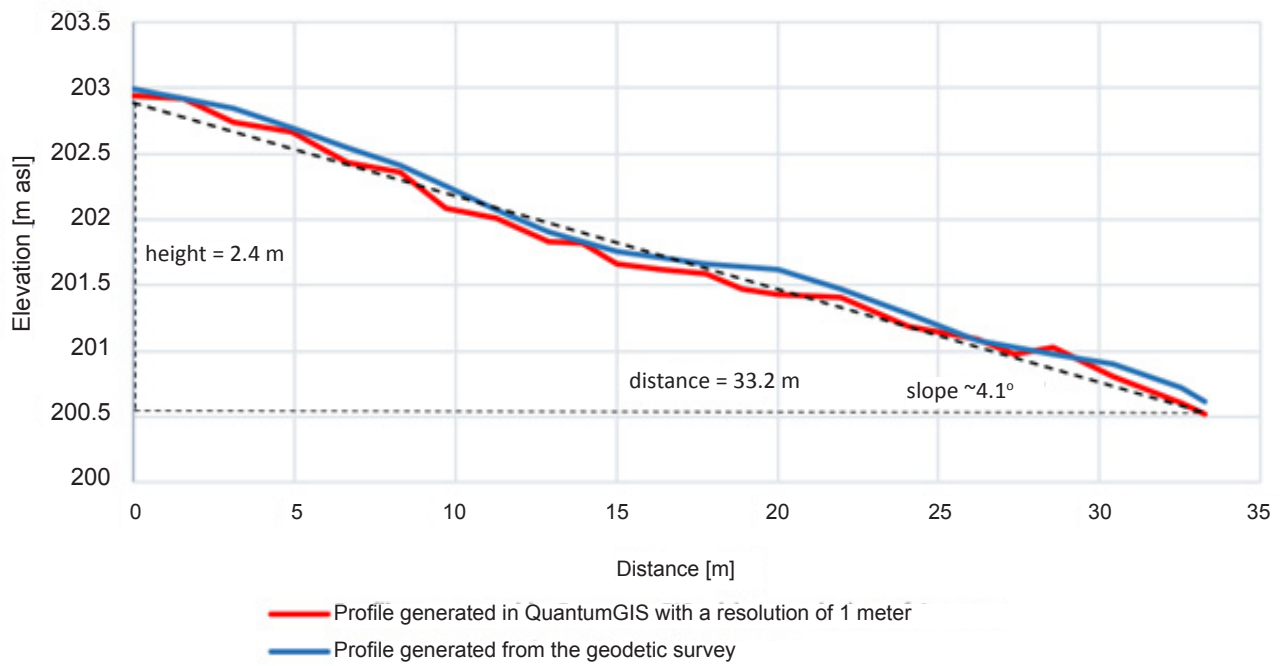


Figure 24. Comparison profile of slopes for spatial resolution 1 meter with survey data collection, which was made by a tachymeter (authors' own study).

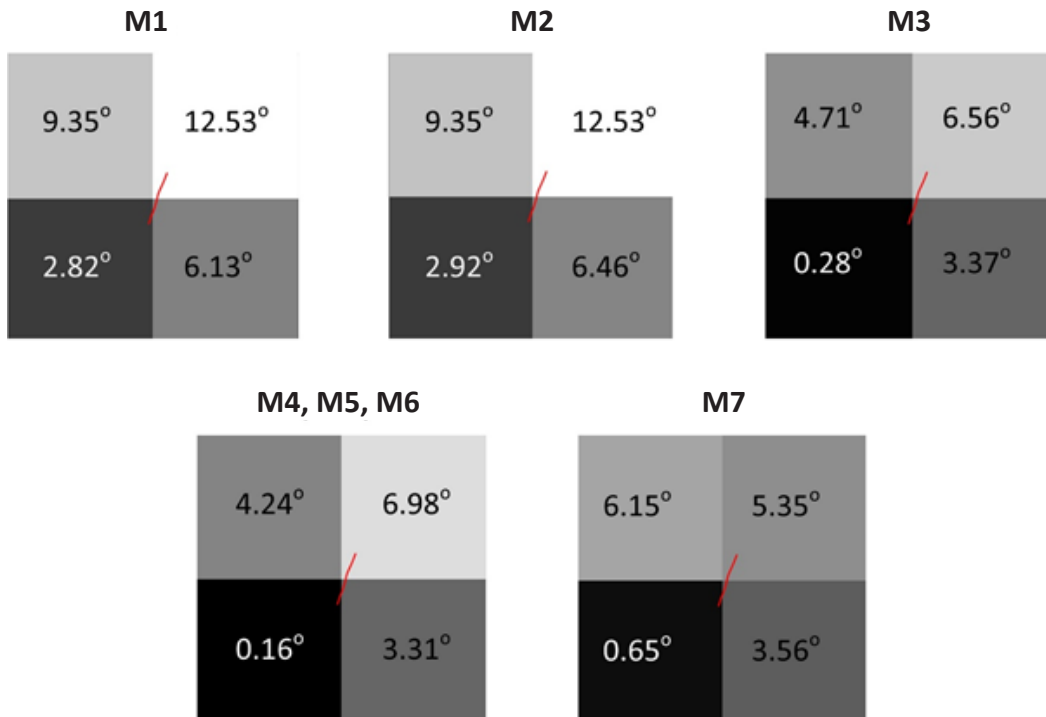


Figure 25. Slopes calculated using various methods for 90 meters resolution (authors' own study).

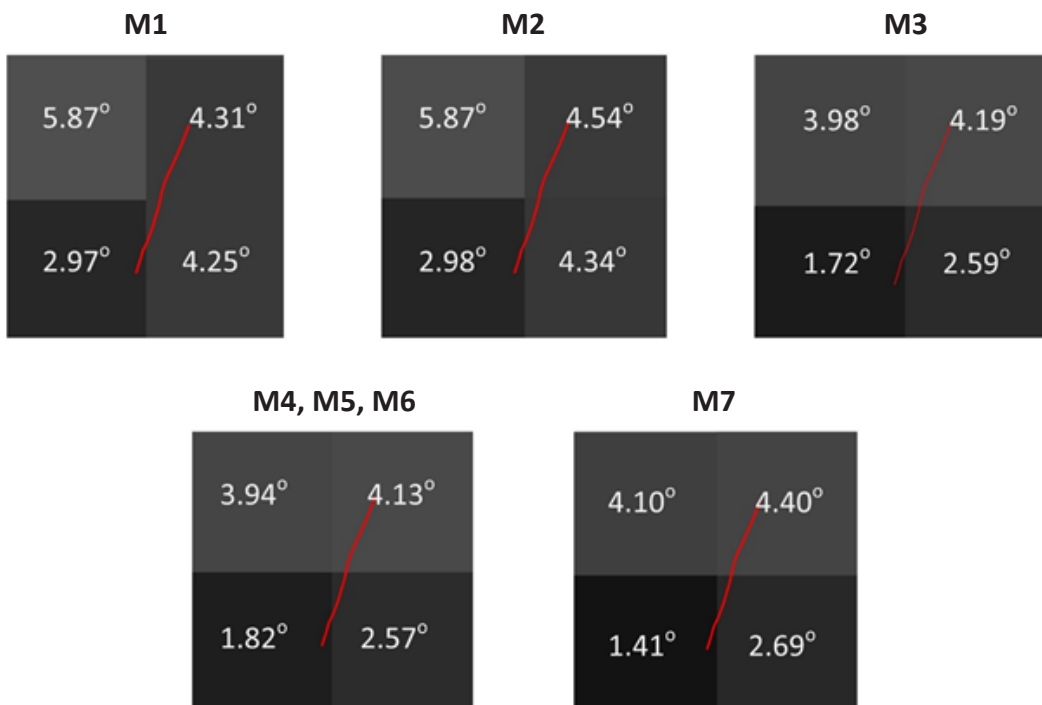


Figure 26. Slopes calculated using various methods for 30 meters resolution (authors' own study).

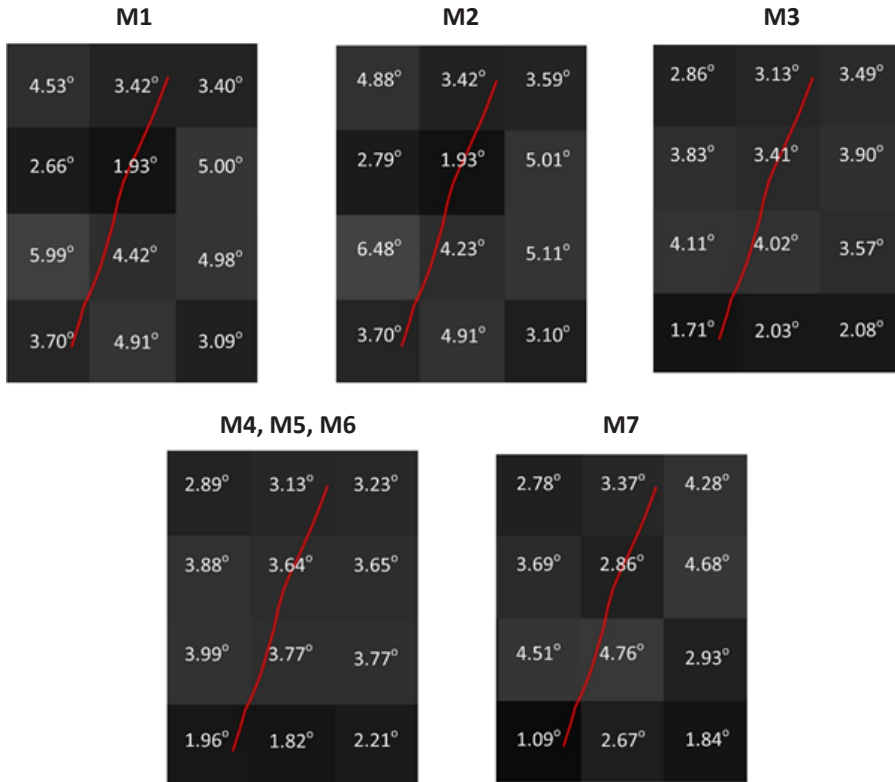


Figure 27. Slopes calculated using various methods for 10 meters resolution (authors' own study).

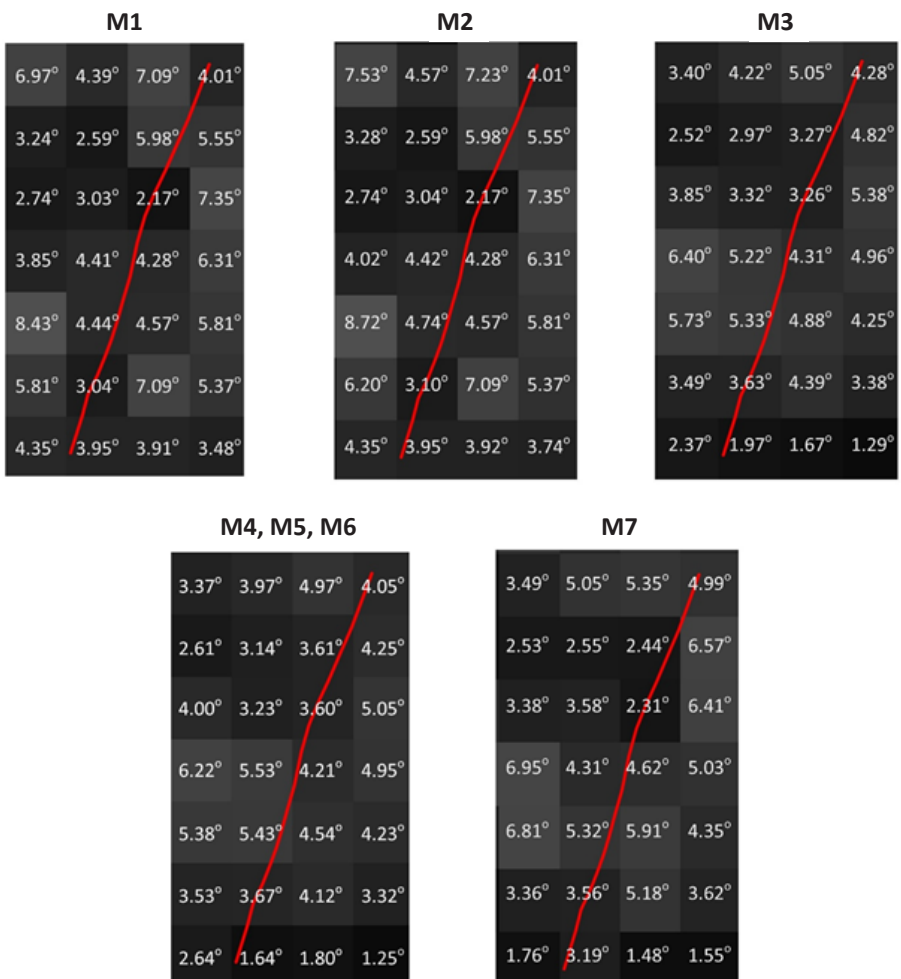


Figure 28. Slopes calculated using various methods for 5 meters resolution (authors' own study).

share is approximately 4% lower at 50.5%, while for the 3.00°–5.99° interval the pixel share is approximately 3% higher at 29%.

The M7 method uses an equation with 9 parameters to calculate indicators. It is more general than other methods using 6 parameters and more flexible (Singer, 2015). The above method (M7) represents the slope gradients well when compared to the actual geodetic field survey for different resolutions. However, a more thorough analysis of the above methods would need to be carried out for geodetic measurement in other parts of the catchment to reliably determine which of the described methods is most suitable for calculating slope gradients. Furthermore, according to Cadell's research (Cadell, 2002), the 2nd Degree Polynomial Adjustment (M7) method is better for less varied relief (smoother surfaces). In contrast, the Third-order Infinite Method for Calculating Slope (M3) can be used for more rough surfaces. Also in a study by García Rodríguez and Giménez Suárez (2010), the 2nd Degree Polynomial Adjustment method (M7) was shown to be the recommended algorithm for determining slope angles.

The correct calculation of land slopes is an important aspect in spatial planning using GIS tools. This allows for the delimitation of suitable areas for development, as well as problem areas with a higher slope, whose inappropriate designation, e.g. as arable land, can generate ongoing costs (Sałata, Prus, 2012).

A study on the effect of DTMs with different resolutions on the accuracy of watercourse line extraction was carried out in the Glinianka watercourse catchment area (Szczepaniak-Kołtun, 2016). GRID models with a resolution of 1 m were used for the study, which were generalised to resolutions of 2, 3, 4 and 5 meters. Watercourse lines were generated for the resulting rasters, which were analysed and compared with the results of direct measurements. The study found that the greatest comparability of the generated watercourse lines to the measured course was obtained for an area with a clearly defined river valley. In contrast, areas with flat, wide valleys are the most difficult to analyse hydrologically (Szczepaniak-Kołtun, 2016).

The influence of resolution and method of elevation data acquisition on the accuracy of DTMs and slope and exposure models was assessed in a study on a section of the Vistula River near Toruń (Burdziej, Kunz, 2006). Based on GRID models, DTMs with resolutions of 1, 5, 10, 25, 50 and 100 meters were generated for 4 data acquisition methods (laser, photogrammetric, level, interferometric). The study shows that decreasing the resolution generalises the model. This contributes to the averaging of values, the loss of extreme values and an increase in the mean error (primarily for slope models). It was also found that the DTM acquisition method only affects the accuracy of the DTM at high resolutions of 1 to 25 m. The authors concluded that the highest possible resolution, preferably 1 m and no less than 10 m, should be used for slope calculations. However, for small-scale studies that do not require high accuracy,

a low resolution of 50 or 100 m can be used. In addition, it has been found that the largest slope errors correspond to landforms with the highest slopes, which are very important in erosion studies (Burdziej et al., 2006).

In this study, resolutions of 1, 5, 10, 30, 90 meters were tested. For 1 m resolution, the variance for all methods varied slightly from 45.9 to 48.5. For 5 m resolution, the variance for M1 and M2 is 38.0–39.2, while for M3–M7 it is 30.2–33.4. There are similar differences for 10 m resolution, where the variance for M1 and M2 is 31.6–32.7, and for M3–M7 is 21.7–25.3. Subsequently, for 30 m, the variance for M1 and M2 is 20.8–21.7, and for M3–M7 is 11.4–14.4. For 90 m, the variance for M1 and M2 is 9.1–9.4, and for M3–M7 is 3.8–5.3 (Table 2). From the above results, it can be concluded that resolutions below 30 m represent terrain variability well, showing a large variation in slope, reflecting real landscape better. For resolutions above 30 m, this variation is much smaller and may be insufficient for different surveys. At the same time, the results for the different percentage intervals at resolutions of 5, 10 and 30 m in Figures 16–20 are similar to each other. Data indicate that when preparing DTMs for studies involving terrain features, resolutions below 30 m should be used. Due to the optimum processing speed of the data and the very good terrain representation, a resolution of 5 m seems to be the optimum solution that can be used for further studies of the Bystra river catchment.

CONCLUSIONS

Studies have shown that a good reproduction of the actual relief, represented by a DTM with a resolution of 1 m, deteriorates significantly starting from a resolution of 30 m. The method for determining land slopes that reproduces most accurately the actual relief variation is Third-order Infinite Method for Calculating Slope method (M3) (Horn, 1981).

However, the literature suggests that the 2nd Degree Polynomial Adjustment method (M7) (Zevenbergen et al., 1987) is more recommended for smooth and rolling terrain. In contrast, the M3 method (Horn, 1981) is considered more suitable for varied landscape relief. In this publication, similar results to the M3 method are shown by methods: 8 Neighbors, Even Weighting Evans (M4) (Evans, 1979), 8 Neighbors, Even Weighting Heerdegen method (M5) (Heerdegen, Beran, 1982), Braunschweiger Relief Model (M6) (Bauer et al., 1985). Therefore, it is also possible to use these methods for rougher terrain. For the Bystra catchment in question, the M3 method would be best due to the varied relief with numerous gullies.

The results of the analyses are crucial for determining the minimum quality of the DTM data in terrain-oriented studies, eg. simulations on hydrology, soil erosion etc. The quality of the DTM data is closely related to its resolution. In many cases, the resolution of the data determines the respective quality of the results and their suitability for fur-

ther analysis. In this study, high resolution data (less than 30 m) were found to be suitable for the analysis and interpretation of slope gradients in a small catchment. The optimum resolution to be used for further studies within Bystra catchment is 5 m. This is an appropriate resolution due to the very good data quality while assuring good processing speed on the computer.

The study reveals that the lowest acceptable resolution in terms of adequate representation of terrain slopes to be used in studies on an upland catchment of Bystra river is 30 m. The use of DTMs with adequate resolution remains a crucial prerequisite for valid morphometric, geomorphological or hydrological studies of small catchments, where the quality of the results is important, e.g. in accurate catchment water balance analysis or soil erosion analysis in agriculture.

REFERENCES

- Badora D., Wawer R., Nierobca A., Krol-Badziak A., Kozyra J., Jurga B., Nowocien E., 2022.** Modelling the hydrology of an upland catchment of Bystra river in 2050 climate using RCP 4.5 and RCP 8.5 emission scenario forecasts. *Agriculture*, 12(3): 403, doi: 10.3390/agriculture12030403.
- Baran-Zglobicka B., Gawrysiak L., Warowna J., Zglobicki W., 2011.** The importance of relief in the process of spatial planning within upland areas. *Czasopismo Techniczne, Architektura/Technical Transactions, Architecture*. Wydawnictwo Politechniki Krakowskiej, 6-A, zeszyt 14, rok 108, 17: 102-106. (in Polish + summary in English)
- Bauer J., Rohdenburg H., Bork H.-R., 1985.** Ein Digitales Reliefmodell als Voraussetzung fuer ein deterministisches Modell der Wasser- und Stoff-Fluesse. *Landschaftsgenese und Landschaftsoekologie*, H.10, Parametereaufbereitung fuer deterministische Gebiets-Wassermodelle, Grundlagenarbeiten zu Analyse von Agrar-Oekosystemen, eds.: Bork H.-R., Rohdenburg H., pp. 1-15.
- Burdziej J., Kunz M., 2006.** Estimation of resolution influence and methods of acquiring high-altitude data on the accuracy of numeric terrain models and models of slopes and aspects. *Archiwum Fotogrametrii, Kartografii i Teledetekcji*, 16: 111-123. (in Polish + summary in English)
- Cadell W., 2002.** Report on the generation and analysis of DEMs for spatial modelling. <https://macaulay.webarchive.hutton.ac.uk/LADSS/documents/DEMs-for-spatial-modelling.pdf> (accessed 10.09.2022).
- CODGiK, 2013. Centralny Ośrodek Dokumentacji Geodezyjnej i Kartograficznej, <http://www.gugik.gov.pl/pzgi/zamow-dane/numeryczny-model-terenu> (accessed 02.02.2017)
- Dixon B., Uddameri V., 2016.** GIS and Geocomputation for Water Resource Science and Engineering. 10.1002/9781118826171, ISBN: 978-1-118-35413-1, John Wiley & Sons, p. 568, New Jersey, p. 193-194
- Drzewiecki W., Mularz S., Pirowski T., 1999.** Generating slope and aspect maps using different GIS packages. http://home.agh.edu.pl/~zfiit/publikacje_pliki/Drzewiecki_Mularz_Pirowski_1999.pdf (accessed 10.03.2017). (in Polish + summary in English)
- Evans I.S., 1979.** An integrated system of terrain analysis and slope mapping. Final report on grant DA-ERO-591-73-G0040. University of Durham, England.
- García Rodríguez J.L., Gimenez Suarez M.C., 2010.** Comparison of mathematical algorithms for determining the slope angle in GIS environment. *Aqua-LAC: journal of the International Hydrological Programme for Latin America and Caribbean*, 2: 78-82, http://static1.1.sqspcdn.com/static/f/891472/20388944/1348408686890/Rodriguez_and_Suarez_2010.pdf?token=bVK1FwETz%2BpMZ8wHUuhqTfPwv4%3D (accessed 29.08.2022).
- Heerdegen R.G., Beran M.A., 1982.** Quantifying source areas through land surface curvature. *Journal of Hydrology*, 57: 359-373.
- Hejmanowska B., 2007.** NMT (GRID/TIN) analysis - OKI data example. *Archiwum Fotogrametrii, Kartografii i Teledetekcji*, 17a: 281-289. (in Polish + summary in English)
- Hejmanowska B., Drzewiecki W., Kulesza L., 2008.** The quality of digital terrain models. *Archiwum Fotogrametrii, Kartografii i Teledetekcji*, 18a: 163-175. (in Polish + summary in English)
- Horn B.K., 1981.** Hill shading and the reflectance map. *Proceedings of the IEEE*, 69(1): 14-47.
- Józefaciuk A., Józefaciuk Cz., 1979.** A trial to estimate the wind erosion threatening of the soils in Poland. *Pamiętnik Puławski*, 71: 167-177. (in Polish + summary in English)
- Józefaciuk A., Józefaciuk Cz., 1992a.** Structure of water erosion hazard of physico-geographical units of Poland. *Pamiętnik Puławski*, 101(suplement): 23-50. (in Polish + summary in English)
- Józefaciuk Cz., Józefaciuk A., 1992b.** Gully densities in physico-geographical units of Poland. *Pamiętnik Puławski*, 101(suplement): 51-66. (in Polish + summary in English)
- Moore I.D., Grayson R.B., Ladson A.R., 1991.** Digital terrain modeling – a review of hydrological geomorphological and biological applications. *Hydrological Processes*, 5: 3-30.
- Nicótina L., Tarboton D.G., Tesfa T.K., Rinaldo A., 2011.** Hydrologic controls on equilibrium soil depths. *Water Resources Research*, 47, W04517, 11 p.p., doi: 10.1029/2010WR009538. <https://agupubs.onlinelibrary.wiley.com/doi/full/10.1029/2010WR009538>, accessed 29.08.2022
- Nowocien E., 2008.** Wybrane zagadnienia erozji gleb w Polsce. *Studia i Raporty IUNG-PIB, Puławy*, 10: 9-38.
- O’Callaghan J.F., Mark D.A., 1984.** The Extraction of the Drainage Networks from Digital Elevation Data. *Computer Vision, Graphics, and Image Processing*, 28: 323-344, doi: 10.1016/S0734-189X(84)80011-0.
- Rukundo O., Cao H., 2012.** Nearest neighbor value interpolation. *International Journal of Advanced Computer Science and Applications*, 3(4): 25-30, doi: 10.14569/IJACSA.2012.030405, https://thesai.org/Downloads/Volume-3No4/Paper_5-Nearest_Neighbor_Value_Interpolation.pdf (accessed 09.09.2022).
- SAGA GIS, 2004. System of Automated Geoscientific Analyses, https://saga-gis.sourceforge.io/saga_tool_doc/2.2.5/ta_hydrology_5.html, 29.08.2022
- Salata T., Prus B., 2012.** Areas delimitation for spatial planning. *Acta Scientiarum Polonorum, Administratio Locorum*, 11(3): 215-225, https://bazhum.muzhp.pl/media/files/Acta_Sci

- entiarum_Polonorum_Administratio_Locorum/Acta_Scientiarum_Polonorum_Administratio_Locorum-r2012-t11-n3/Acta_Scientiarum_Polonorum_Administratio_Locorum-r2012-t11-n3-s215-225/Acta_Scientiarum_Polonorum_Administratio_Locorum-r2012-t11-n3-s215-225.pdf (accessed 05.06.2022). (in Polish + summary in English)
- Salata T., 2015.** Synteza jakości rolniczej przestrzeni produkcyjnej. http://matrix.ur.krakow.pl/~tsalata/zpg/zmpred.php?akcja=studium_spadkow, (accessed 03.04.2017)
- Singer M., 2015.** Enhanced Wetness Modeling in SAGA GIS, http://gracilis.carleton.ca/CUOSGwiki/index.php/Enhanced_Wetness_Modelling_in_SAGA_GIS, (accessed 05.08.2017)
- Slope algorithm, 2015, https://www.usna.edu/Users/oceanography/md_help/html/demb1f3n.htm, (accessed 29.08.2022)
- Smith M., Goodchild M., Longley P., 2015.** Geospatial Analysis, A comprehensive guide to principles – Techniques and software tools. http://www.spatialanalysisonline.com/HTML/index.html?d-infinity_model.htm, (accessed 04.03.2017)
- Stateczny A., Łogasz K., 2007.** Aspekty tworzenia Numerycznego Modelu Terenu na podstawie skaningu laserowego – LIDAR. Wykład, 15.06.2007, https://www.geosystems.pl/upload/zalaczniki/KNT_2007%20-%20Aspekty%20Tworzenia%20Numerycznego%20Modelu%20Terenu%20na%20Podstawie%20Skaningu%20Laserowego%20-%20LIDAR%20-%20Stateczny%20A,%20Logasz%20K.pdf (accessed 05.06.2022)
- Szczepaniak-Koltun Z., 2016.** Assessment of DTM resolution influence on the accuracy of flow lines extraction. *Archiwum Fotogrametrii, Kartografii i Teledetekcji*, 28: 115-124, doi: 10.14681/afkit.2016.009. (in Polish + summary in English)
- Tang J., Pilesjö P., 2011.** Estimating slope from raster data: A test of eight different algorithms in flat, undulating and steep terrain. *WIT Transactions on Ecology and the Environment*, 146: 143-154, doi: 10.2495/RM110131, <https://www.witpress.com/Secure/elibrary/papers/RM11/RM11013FU1.pdf> (accessed 29.08.2022).
- Tarboton D.G., 1997.** A new method for the determination of flow directions and upslope areas in grid digital elevation models. *Water Resources Research*, 33(2): 309-319, <https://agupubs.onlinelibrary.wiley.com/doi/pdf/10.1029/96WR03137>, doi: 10.1029/96WR03137 (accessed 29.08.2022).
- Travis M.R., Elsner G.H., Iverson W.D., Johnson C.G., 1975.** VIEWIT: computation of seen areas, slope, and aspect for land-use planning, USDA F.S. Gen. Tech. Rep. PSW-11/1975, 70 pp., Berkeley, California, U.S.A.
- Urbański J., 2012.** GIS w badaniach przyrodniczych. http://ocean.u.g.edu.pl/~oceju/CentrumGIS/dane/GIS_w_badaniach_przyrodniczych_12_2.pdf (accessed 07.03.2017).
- Wawer R., Nowocień E., Podolski B., 2010.** Actual water erosion risk in Poland based upon Corine Land Cover 2006. *Electronic Journal of Polish Agricultural Universities. Series Environmental Development*, 13(2), available online: <http://www.ejpau.media.pl/volume13/issue2/art-13.html> (accessed 07.03.2017).
- Wawer R., Nowocień E., 2018.** Erozja wodna i wietrzna w Polsce. *Studia i Raporty IUNG-PIB*, 58(12): 57-79, https://iung.pl/sir/zeszyt58_5.pdf (accessed 05.06.2022).
- Weih R.C. Jr., Mattson T.L., 2004.** Modeling Slope in a Geographic Information System. *Journal of the Arkansas Academy of Science*, 58: 100-108, <https://scholarworks.uark.edu/cgi/viewcontent.cgi?article=1578&context=jaas> (accessed 29.08.2022).
- Wieczorek M., Żyszkowska W., 2011.** The Morphometric Relief Characteristic on a Basis of Digital Terrain Models. *Polski Przegląd Kartograficzny*, 43(2): 130-144. (in Polish + summary in English)
- Zachar D., 1982.** Soil erosion. *Developments in soil science*, vol. 10, Elsevier scientific publishing company, Amsterdam, Oxford, New York, 544 pp.
- Zevenbergen L.W., Thorne C.R., 1987.** Quantitative analysis of land surface topography. *Earth Surface Processes and Landforms*, 12(1): 47-56, doi: 10.1002/esp.3290120107.

| Author | ORCID |
|---------------|---------------------|
| Damian Badora | 0000-0002-2497-8500 |
| Rafał Wawer | 0000-0001-9266-9577 |

received – 18 February 2021
revised – 19 November 2022
accepted – 28 November 2022

The authors declare no conflict of interest.



This article is an open access article distributed under the terms and conditions of the Creative Commons Attribution-ShareAlike (CC BY-SA) license (<http://creativecommons.org/licenses/by/4.0/>).